NASA TECHNICAL NOTE

ACOUSTIC AND AERODYNAMIC PERFORMANCE OF A VARIABLE-PITCH 1.83-METER- (6-FT-) DIAMETER 1.20-PRESSURE-RATIO FAN STAGE (QF-9)

Frederick W. Glaser, Richard P. Woodward, and James G. Lucas

Lewis Research Center
Cleveland, Ohio 44135

NATIONAL AERONAUTICS AND SPACE ADMINISTRATION • WASHINGTON, D. C. • FEBRUARY 1977

1. Report No.	2. Government Accession No.	3. Recipient's Catalog No.
NASA TN D-8402		

4. Title and Subtitle: ACOUSTIC AND AERODYNAMIC PERFORMANCE OF A VARIABLE-PITCH 1.83-METER- (6-FT-) DIAMETER 1.20-PRESSURE-RATIO FAN STAGE (QF-9)

5. Report Date: February 1977

6. Performing Organization Code:

7. Author(s): Frederick W. Glaser, Richard P. Woodward, and James G. Lucas

8. Performing Organization Report No.: E-8837

9. Performing Organization Name and Address:
Lewis Research Center
National Aeronautics and Space Administration
Cleveland, Ohio 44135

10. Work Unit No.: 505-03

11. Contract or Grant No.:

12. Sponsoring Agency Name and Address:
National Aeronautics and Space Administration
Washington, D.C. 20546

13. Type of Report and Period Covered: Technical Note

14. Sponsoring Agency Code:

15. Supplementary Notes:

16. Abstract

Far field noise data and related aerodynamic performance are presented for a variable pitch fan stage having characteristics suitable for low-noise, STOL engine application. However, no acoustic suppression material was used in the flow passages. The fan was externally driven by an electric motor. Tests were made at several forward thrust rotor blade pitch angles and one for reverse thrust. Fan speed was varied from 60 to 120 percent of takeoff (design) speed, and exhaust nozzles having areas 92 to 105 percent of design were tested. The fan noise level was at a minimum at the design rotor blade pitch angles of 64° for takeoff thrust and at 57° for approach (50 percent takeoff thrust). Perceived noise along a 152.4-m (500-ft) sideline reached 100.1 PNdB for the takeoff (design) configuration for a stage pressure ratio of 1.17 and thrust of 57 600 N (13 000 lbf). For reverse thrust the PNL values were 4 to 5 PNdB above the takeoff values at comparable fan speeds.

17. Key Words (Suggested by Author(s))	18. Distribution Statement
Fan noise Noise reduction Short takeoff aircraft	Unclassified - unlimited STAR Category 02

19. Security Classif. (of this report)	20. Security Classif. (of this page)	21. No. of Pages	22. Price*
Unclassified	Unclassified	66	A04

* For sale by the National Technical Information Service, Springfield, Virginia 22161

CONTENTS

ACOUSTIC AND AERODYNAMIC PERFORMANCE OF A VARIABLE-PITCH 1.83-METER- (6-FT-) DIAMETER 1.20-PRESSURE-RATIO FAN STAGE (QF-9)

by Frederick W. Glaser, Richard P. Woodward, and James G. Lucas

Lewis Research Center

SUMMARY

This report presents the acoustic and aerodynamic performance for a 1.83-meter- (6-ft-) diameter experimental fan stage with characteristics suitable for a low-noise STOL engine. The fan was externally driven by an electric motor. Low noise features included the elimination of inlet guide vanes, low rotor tip speed (213.2 m/sec (700 ft/sec)), large axial spacing between the rotor and stator blade rows (two rotor mean chord lengths), and a low number of rotor blades (15) which placed the fundamental blade passage frequency in a lower frequency, lower annoyance region of the spectrum. The fan had no acoustic suppression in the flow passages.

The fan features adjustable-pitch rotor blades which provided a means for testing at several forward thrust blade setting angles as well as one for reverse thrust.

The tests were made at fan speeds from 60 to 120 percent of design speed, and the aerodynamic loading was varied by using exhaust nozzles having 92, 95, 100, and 105 percent of design nozzle area.

The fan stage operated somewhat below design-predicted values of mass flow and pressure ratio. The aerodynamic results indicate that performance can be improved by either running the fan at speeds above its takeoff (design) speed, increasing the fan pitch angle, or decreasing the fan exhaust nozzle area below its design area.

The fan noise level was at a minimum at the design rotor blade pitch angle (64°) for takeoff thrust and at 57° for approach (50 percent of takeoff thrust). The perceived noise along a 152.4-meter- (500-ft-) sideline was exhaust quadrant dominated and reached 100.1 perceived noise decibels (PNdB) for the takeoff (design) configuration, which had a stage pressure ratio of 1.17 and thrust of 57 600 newtons (13 000 lbf). For reverse thrust the perceived noise level values are 4 to 5 PNdB above takeoff results at comparable fan speeds.

INTRODUCTION

Short takeoff and landing (STOL) aircraft are being considered for operation in highly populated areas and in developing countries with inadequate highway systems. Although no firm noise specifications exist at present for STOL aircraft that are comparable to Federal Air Regulation - Part 36 (FAR-36), a much-used goal for STOL sideline noise is 95 effective perceived noise decibels (EPNdB) along a 152.4-meter- (500-ft-) sideline (ref. 1). This noise level is for the entire aircraft and will dictate single-engine levels somewhat below this value. The reduction of engine noise is therefore an important consideration in the engine design. An engine suitable for a quiet STOL application would require a large air flow with relatively low exhaust velocity resulting in a bypass ratio of about 10 to 15 (ref. 2) and a fan pressure ratio of 1.20 to 1.35.

This report presents the acoustic and aerodynamic performance of a full-scale experimental variable-pitch fan with characteristics suitable for a low-noise STOL engine. The tests were conducted in the full-scale fan acoustic test facility at the Lewis Research Center, in which the fans are driven by an electric motor. This 1.83-meter- (6-ft-) diameter fan, designated QF-9, was designed and fabricated under contract for the Lewis Research Center by the Hamilton-Standard Division of the United Technologies Corporation. The fan stage incorporated features for low noise including the elimination of inlet guide vanes, low rotor-blade-tip speed, large axial spacing between the rotor and stator blade rows, and low number of rotor blades. The low number of rotor blades (15) was expected to yield a noise benefit by reducing the frequency of the blade passing tone which would be reflected in a lower calculated perceived noise level (PNL). In addition, the fan featured adjustable-pitch rotor blades. Although primarily incorporated for thrust reversal considerations, the adjustable-pitch feature provided a means of optimizing the thrust-noise relation for changing flight conditions (i.e., takeoff and landing). The fan stage was designed for a pressure ratio of 1.20 and a rotor tip speed of 213.3 meters per second (700 ft/sec).

The QF-9 fan was run without acoustic suppression in the flow passages. The configuration tested included four exhaust nozzle sizes: the design takeoff nozzle, nozzles with 95 and 92 percent of design nozzle area, and one nozzle with no exhaust contraction resulting in an exit area 105 percent of design.

A scale model of fan QF-9 with a 50.8-centimeter (20-in.) rotor tip diameter was extensively tested for aerodynamic performance in a highly instrumented indoor facility (refs. 3 and 4). Selected results from these tests are compared to those obtained for the full-scale QF-9 fan. Also, in this report optimum blade pitch angles are defined which minimize noise at takeoff and approach conditions. Included are results for a reverse thrust configuration. Data are compared with a noise prediction method. Broadband and tone components of the one-third-octave analysis are considered in analyzing the fan

acoustic performance.

The acoustic results for QF-9 are presented in terms of sound pressure level (SPL), sound power level (PWL), and perceived noise level (PNL). Complete one-third-octave data are presented in tabular form in reference 5.

FAN DESIGN

Acoustic and Aerodynamic Considerations

Fan QF-9, a 1.20-pressure-ratio experimental fan stage, was designed to have characteristics typical of the type of fan which might be used in a turbofan engine for an externally blown flap, engine under-the-wing STOL aircraft. This fan was designed to be quiet within the constraints of conservative, conventional aerodynamic design practice. Among the acoustic considerations in the design are the absence of inlet guide vanes, the low rotor-blade tip speed, and the large axial spacing between the rotor and stator blade rows. These features have been used before in low-noise fans (ref. 6) and are compatible with low-noise design practice. In addition, the QF-9 featured manually adjustable pitch rotor blades.

Inlet guide vanes were omitted from the QF-9 fan because they produce a pattern of wakes at their trailing edges which impinge on the rotor blades, and thus cause emission of noise at the blade-passing frequency (ref. 7).

The low design pressure ratio could be achieved with rotor-blade-tip speeds which were low enough to avoid supersonic relative Mach numbers at the rotor blade tip. Thus, the generation of multiple pure tones was not expected.

The fan stage was designed with a small number of rotor blades and stator vanes with relatively large chords. The use of a low number of rotor blades in the fan design was advantageous in reducing the frequency of the blade passage tone to a lower annoyance region of the audio spectrum. Reference 8 indicates that long stator chords reduce the response to incoming rotor wakes, possibly reducing the blade passing frequency noise. The final contractor design resulted in 15 rotor and 11 stator blades (ref. 9).

The axial spacing between the rotor and stator blade row was made as large as reasonably possible (two rotor chords at the mean radius, ref. 9) in an effort to reduce rotor/stator interaction noise. This large spacing provides mixing length for the rotating wake pattern to dissipate significantly before impinging on the stator vanes. This impingement on the stators causes the emission of sound at blade-passing frequency. With the rotor wakes largely dissipated as a result of the large spacing and with no inlet-guide-vane wakes, a reduction in blade-row-interaction noise generation at blade-passing frequency was expected (ref. 10).

Low-noise fans are frequently designed with consideration of the "cutoff" theory of reference 11 to prevent the forward propagation of certain spinning modes. This technique requires the number of stator vanes to be slightly greater than twice the number of rotor blades. Fan QF-9 did not include the necessary number of stator vanes required to acoustically cutoff the blade-passing frequency fundamental because of stator solidity considerations.

Stage Design Parameters

A brief description of the more important features of the design is given here. In tables I and II and reference 9, selected stage design configuration parameters are given for fan QF-9. At the design rotor tip speed the rotor tip inlet relative Mach number is 0.865, somewhat less than that which would be expected to generate significant multiple pure tones (ref. 12).

The energy input to the air by the rotor blades is a function of both rotor-blade-tip speed and blade loading. Local blade loading is frequently expressed in terms of the diffusion factor (D-factor), which is based on the diffusion in velocity on the blade suction surface. QF-9 had a design rotor tip speed of 213.3 meters per second (700 ft/sec) and a maximum rotor diffusion factor of 0.53. At the rotor hub and tip the diffusion factors were 0.53 and 0.43, respectively. These values for the diffusion factors are near the generally used upper limit of 0.50 to 0.55, thus indicating that the fan QF-9 rotor is relatively highly loaded.

Figures 1 and 2 are photographs of the fan rotor and stator blading. Figure 1 shows a partial downstream view of the 15-blade rotor assembly. The rotor chord increases from hub to tip, with a maximum value of 34.3 centimeters (13.5 in.) at the tip. The partial upstream view of the 11-blade (constant chord) stator assembly (fig. 2) shows the very low solidity, large chord blading. Stator outflow was designed for the axial direction.

The already existing structure also required axial stator outflow for fan QF-9. The axial requirement was imposed by the centerbody support pylon shown in figure 2. The pylon is a 20 percent thick airfoil in cross section. Any significant angularity of the flow impinging on it would cause a large local flow separation which would in turn block a portion of the flow path in this area and thus cause the fan to operate closer to stall.

Figure 3 compares the design rotor tip speed and stage pressure ratio of several fans tested at the Lewis quiet fan facility. The lines of constant work coefficient give an indication of the overall stage loading and show the fan QF-9 stage to have relatively high loading. Fans QF-6 (ref. 13) and QF-8 (ref. 14) were also experimental STOL application fans. Fan QF-9 had the lowest tip speed and highest work coefficient of the three STOL fans. The remaining fans presented in figure 3 are more suited for conven-

tional takeoff and landing aircraft.

Flow Path Parameters

The QF-9 design had an inlet hub-tip ratio of 0.46. The flow passage was designed to have no inner- or outer-radius convergence through the rotor. This was necessary to allow the rotor blades to rotate to a reverse thrust blade pitch angle. The rotor blade tips were contoured to provide adequate clearance for adjusting the rotor blades. This straight inner flow passage is shown in the stage cross section (forward thrust) (see fig. 4).

The QF-9 fan was designed to be tested using part of the already existing structure and exhaust-end flow ducting of the full-scale fan facility. The flow passage was designed to have a single flow path. As a result, the fan rotor discharge flow was not divided radially (see fig. 4) as would be the case in an actual turbofan engine where the inner portion of the rotor flow is ducted into the core engine. The inner radius of the flow passage of the full-scale fan QF-9 was decreased downstream of the stator (fig. 4) to compensate for support pylon blockage (fig. 2).

Figure 5 shows the nozzle modification and instrumentation locations for reverse thrust. The through-feather mode of rotor blade reversal was selected because of the high levels of reverse thrust measured in the scale-model wind tunnel fan tested referred to in reference 15. As may be seen in the sketch in figure 6, this mode of thrust reversal results in the more aerodynamically preferred blade orientation with respect to blade camber.

Figure 7, a cutaway sketch of the QF-9 fan installation as tested at the Lewis quiet fan facility, shows the drive shaft in the fan inlet, relative positions of rotor and stator blades, and the support pylon. In all testing the fan flow passage had no acoustic suppression treatment.

TEST CONFIGURATIONS AND DATA ANALYSIS

A tabulation of the configurations for which aerodynamic and acoustic data are reported is given in table III. Four separate exhaust nozzle configurations were used. These were referred to as design takeoff, 95 and 92 percent of design, and 105 percent of design. The design nozzle had an exit area of 2.02 square meters (21.75 ft^2).

The adjustable-pitch rotor was tested at six forward and one reverse thrust rotor blade pitch angles. These angles, listed in table III, are measured from the tangential direction (consistent with manufacturing specifications) at the 75 percent blade radius (i.e., measured from the rotor axis). In the reverse-thrust configuration the incoming

air stream entered through the exhaust nozzle which was flared open (45^{o}) to form a contracting flow path. The exit air flow left the fan through the bellmouth, was discharged over the drive shaft, and was deflected from the drive motor building by a blast shield (see fig. 8(b)). Results are given with and without this shield (table III). In the reverse mode the stators acted like negative-camber inlet guide vanes whose wakes impinged on the rotor blades, hence a likely noise source.

Facility

The QF-9 fan is shown installed at the outdoor full-scale quiet fan facility in figure 8. The forward thrust installation is shown in figure 8(a), while figure 8(b) shows the reverse thrust installation with the blast deflector in place. Existing wind tunnel drive motors were used to drive the fan through a gearbox and drive shaft.

Figure 9 is a plan view of the test site. The entire test site surface was asphalt. The acoustic far-field data were taken with an array of microphones located at the fan centerline elevation of 5.9 meters (19.3 ft) on a 30.5-meter (100-ft) radius from the fan at 10^{o} increments from 10^{o} to 160^{o} from the fan inlet centerline. The center of the microphone array was located 37 meters (121 ft) from the face of the drive motor building. Data were not taken at 0^{o} because of the drive shaft, nor were data taken at angles greater than 160^{o} because of the high-velocity fan exhaust. In figure 8(a) the microphones are shown covered with plastic bags to protect them from the weather. The bags are removed during operation. Additional details on design of the quiet fan facility are given in reference 16. Foam treatment is shown on the portion of the drive motor building wall that was considered likely to cause a sound reflection problem at the nearer microphone locations.

Aerodynamic Instrumentation

To obtain fan aerodynamic performance, measurements were made at four axial locations for forward thrust and one axial location for reverse thrust. Figure 4 shows the four axial locations for forward thrust. The detailed layout of the instrumentation at each of these four measuring stations is shown in figure 10. Six equally spaced iron-constantan thermocouples were located on the bellmouth lip to determine the average inlet total temperature. These thermocouples extended about 1 centimeter from the surface to measure the ambient air temperature. Six static taps were located in the outer wall of the inlet duct. These static taps were used for the inlet mass flow calculation using the assumptions of uniform one-dimensional flow, zero total pressure loss at the duct station, and a zero wall boundary layer thickness. The location of this station was es-

tablished from a potential flow calculation. For the inlet mass flow calculations, the barometric ambient pressure reading was used for total pressure.

Four identical total pressure and temperature rakes were used downstream of the stator blade row to determine the stage exit mass flow and mass-average stage total pressure ratio. Iron-constantan thermocouples were used on these rakes. These rakes were located nominally at 90° intervals but were displaced slightly in order to avoid being in a stator wake. Just downstream of the nozzle exit, three equally spaced total pressure rakes were used for exit momentum or thrust calculations. All rakes were removed for acoustic tests.

The outer wall static taps at the stator discharge station were used in the reverse-thrust configuration (fig. 5) for the mass flow calculation using the assumptions of uniform one-dimensional flow. No aerodynamic rakes were used for reverse thrust tests. For the mass flow calculations, the ambient pressure and temperature readings were used for total pressure and temperature.

The aerodynamic data were recorded through a pressure multiplexing valve, pressure transducer, and data acquisition network. All temperatures were recorded by the same network which takes one scan of aerodynamic pressures and temperatures in approximately 10 seconds. Nine consecutive scans were made at each data point, with the raw data samples arithmetically averaged and used to compute the desired flow parameters. Two separate points were taken at each test condition of speed and configuration. The arithmetic average of the computed parameters are presented in this report.

The appendix presents the equations used to reduce the aerodynamic results. Performance parameters were corrected to standard day conditions of a temperature of 15° C and an atmospheric pressure of 101 325 pascals (760 mm of mercury).

Acoustic Instrumentation

Data acquisition system. - As mentioned previously, far field acoustic measurements were made outdoors with microphones located on the horizontal centerline of the fan 5.9 meters (19.3 ft) above ground. The test site surface was asphalt. The 16 far-field microphones were located on a 30.5-meter (100-ft) radius (fig. 9), except for the 120° and 160° microphone distances which were actually at 31.4 and 31.9 meters, respectively, because of the presence of a walkway through the microphone field. Data from the microphones were corrected to the 30.5-meter (100-ft) radius. The microphone angular positions were measured from the normal fan inlet axis for both forward and reverse thrust configurations. In making the noise measurements, 1.3-centimeter-(0.5-in.-) diameter condenser microphones were used which had sensitivities of -60 decibels relative to 1 volt per microbar. The frequency response of the system, as a whole, was flat from 50 hertz through 20 kilohertz.

The acoustic data were reduced on-line through one-third-octave filters and recorded on magnetic tape for further analysis. Prior to the set of tests for each configuration, a pistonphone signal was impressed on each far-field microphone for absolute calibration.

One-third-octave band analysis. - The one-third-octave band analyzer used for on-line data reduction employed a 4-second averaging time and was stepped sequentially through the angles from 10^{o} to 160^{o}. The 4-second averaging time was selected to accommodate all angles within a 100-second recording while preserving analyzer repeatability. Three separate samples were taken for each data point and averaged.

Results of one-third-octave band sound pressure levels (SPL) analysis yielded data taken under ambient conditions of the test day at the microphone locations. The data were referred to the sound source (i.e., the effect of atmospheric absorption was removed) by computing atmospheric absorption for the test conditions over the propagation path and adjusting the data accordingly. Atmospheric absorption was computed by using continuous frequency-dependent functions derived from reference 17. For the QF-9 spectra, which contained significant fan noise as well as some jet noise, the general shape of each measured spectrum was accounted for and the one-third-octave band attenuations were obtained by integrating the continuous absorption functions over each band (ref. 18).

For power calculations, the SPL's were presumed to be axisymmetric and were integrated over an enclosing hemisphere. Implicit in this procedure was a perfectly reflective ground plane in the sense that acoustic intensity was doubled in the far field. No corrections were made for signal interference effects at the microphones because of ground reflections.

Calculations of atmospheric absorption for a standard day of 15^{o} C and 70-percent relative humidity were made using the data referred to the source and the data so adjusted to standard-day conditions. All one-third-octave band SPL data reported herein are adjusted to standard-day conditions.

The perceived noise values were calculated (ref. 19) from the standard-day data. The perceived noise values take into consideration the frequency-dependent sensitivity of human hearing, thus giving an indication of the human annoyance of the fan noise. For the sideline PNL determinations, the data were adjusted to a 152.4-meter (500-ft) sideline.

Narrow-band analysis. - A fine-resolution, constant-bandwidth analysis shows more detail of the SPL spectra than is possible with the one-third-octave analysis. Narrow-band spectra of selected data were obtained using the magnetic tape recorded data. The effective bandwidth of this spectra is 32 hertz for a 10-kilohertz total range and 3.2 hertz corresponding to a 1-kilohertz range. It should be noted that these spectra were not adjusted in any way and present the signals at the microphones under test-day conditions.

AERODYNAMIC PERFORMANCE

The quiet fan facility was designed primarily for acoustic testing of full-scale fans. The aerodynamic instrumentation, as described, was limited to obtaining an indication of the aerodynamic performance of the fan. Consequently, the aerodynamic results for QF-9 are not as precise as might have been obtained from a specialized aerodynamic test facility such as that of reference 3. Table IV presents a summary listing of selected aerodynamic results for QF-9 for the various configurations which were tested.

Figures 11 and 15 present selected aerodynamic results for QF-9. In general, the aerodynamic results are shown as functions of the percent of corrected fan design speed to facilitate a correlation of these results with the acoustic results.

A conventional fan operating map for fan QF-9 is presented for takeoff (design) rotor blade angle (64^{o}) in figure 11(a) and for approach (50^{o}) in figure 11(b). The stage total pressure ratio is plotted as a function of inlet corrected mass flow to give a series of constant percent speed curves. The model (50.8-cm rotor tip diameter) data of reference 3 were scaled for mass flow differences and also presented on the map for the takeoff rotor angle. An estimated stall line for fan QF-9 is shown on the maps based on the small-scale model results.

The performance map for takeoff (design) rotor angle (fig. 11(a)) of the full-scale fan shows good agreement with the model fan results. The measured values at takeoff (design) speed and design nozzle area of the QF-9 fan stage fell somewhat short of the design-predicted values of weight flow and pressure ratio. The measured weight flow was 388 kilograms per second (855 lbm/sec) as compared to the predicted 403 kilograms per second (889 lbm/sec), and the pressure ratio of 1.17 was less than the predicted 1.20. To achieve a higher pressure ratio, the QF-9 was run at speeds above its takeoff (design) speed. The maximum stage pressure ratio of 1.265 was obtained at 120 percent design speed with the nozzle having 92 percent of design nozzle area.

The performance map for approach rotor angle is shown in figure 11(b). Model data were not available for the 50^{o} rotor angle.

The measured performance values at the designated approach speed (86 percent design) and design nozzle area of QF-9 also fell somewhat short of the design-predicted values of weight flow and pressure ratio. The measured weight flow was 274 kilograms per second (604 lbm/sec) as compared to the predicted 284 kilograms per second (626 lbm/sec), and the pressure ratio was 1.08 as compared to the predicted 1.096. The approach configuration was also run at speeds above approach speed (86 percent of design). The maximum stage pressure ratio of 1.129 was obtained at 100 percent of design speed with the nozzle having 92 percent of design nozzle area.

The overall stage pressure ratio and corrected inlet mass flow shown in figure 11 are plotted as functions of corrected fan speed in figures 12(a) and 13(a), respectively. Figures 12(b) and 13(b) present stage pressure ratio and corrected inlet mass flow for

the design nozzle area for several rotor pitch angles in addition to design (64^{o}) and approach (50^{o}). Manually resetting the blades for a 69^{o} pitch angle increased both pressure ratio and mass flow. The measured pressure ratio at design speed and nozzle area (fig. 12(b)) was 1.188, slightly below design. The measured inlet corrected mass flow was 403 kilograms per second (888 lbm/sec) (fig. 13(b)), essentially the design value.

The stage adiabatic efficiency results obtained for fan QF-9 were low compared to those obtained for the model fan (refs. 3 and 4) and design values. For example, at the design operating condition the measured efficiency was 0.78 - considerably less than the predicted value of 0.90 (table I). This appears to be a facility related problem, perhaps due to recirculated airflow. Since there is this uncertainty in magnitude, the full-scale fan efficiency results are not included with this aerodynamic results presentation. However, the relative levels are believed to be correct and are presented in a later section on acoustic results as an aid in explaining the acoustic behavior of the fan.

For thrust-reversal the rotor blades were manually reset to an angle of 148^{o}. The limited aerodynamic instrumentation for the reverse thrust tests provided for only inlet mass flow measurement. When compared to forward thrust, figure 13(c), the measured inlet corrected mass flow for reverse thrust was reduced at comparable speeds. At 100 percent speed the corrected mass flow was 254 kilograms per second (599 lbm/sec), or about 65 percent of the measured corrected inlet mass flow at takeoff design conditions.

The stage corrected thrust as a function of percent of corrected fan speed (fig. 14(a)) shows that QF-9 at design-point operation developed less than the calculated design corrected thrust of 71 705 newtons (16 120 lbf). The maximum corrected thrust of 79 334 newtons (17 835 lbf) was obtained at 120 percent of takeoff (design) speed with the nozzle having 92 percent of design nozzle area. Figure 14(b) presents corrected thrust for several other forward-thrust rotor pitch angles, including takeoff and approach.

Aerodynamic results indicate that design goals could be approached by an increase in fan design speed, changing the fan pitch angle from 64^{o} to 69^{o}, and decreasing the fan exhaust nozzle area to one having 92 percent of design nozzle area. These results are consistent with the scale model tests of references 3 and 4.

The corrected nozzle exit velocity as a function of inlet mass flow is provided in figure 15 as an aid to the reader who may wish to correlate the jet noise parts of the acoustic results with the fan stage exit velocity.

ACOUSTIC PERFORMANCE

Fan QF-9 was tested at several rotor pitch angles (see table III). While pitch angles were specified for takeoff and approach conditions, it is informative to compare the performance at other blade pitch angles with that observed for the design pitch angles.

This discussion on the fan QF-9 acoustic performance is divided into four main groupings. The first section deals with the acoustics at the design takeoff rotor pitch angle and covers the range of fan speeds and nozzle areas tested. The second section similarly treats the performance at the design approach rotor pitch angle. A comparison of the fan performance at all tested forward-thrust rotor pitch angles is given in the third section, while the fan QF-9 performance at reverse thrust rotor pitch angle is considered in the fourth section.

A complete listing of the fan QF-9 acoustic results and computer plots of selected results are presented in the fan QF-9 data report (ref. 5).

Design Rotor Pitch Angle

Sound pressure level. - The SPL results for fan QF-9 with design nozzle area are presented in figures 16 and 17 at 20° and 130°, respectively, from the fan inlet. The data at these angles are representative of front and rear quadrant results. Figure 16(a) presents the one-third-octave spectra at 20° from the fan inlet at design fan speed and 120 percent of design fan speed. The fundamental blade passing frequency (BPF) and overtone (2 BPF) are well defined in these spectra. The spectrum at 120 percent of fan design speed (256 m/sec, 840 ft/sec) shows a region of multiple pure tones (MPT) at about half of the fundamental blade passing frequency. At this speed the rotor tip relative velocity is 315.2 meters per second (1034 ft/sec), which implies that local regions of near-sonic flow relative to the rotor may exist (see fig. 16(c)).

The constant bandwidth (32 Hz) narrow-band spectra for the results of figure 16(a) are presented in figure 16(b). Again, the blade passing tones and overtones are clearly distinguished in these spectra.

Figure 16(c) gives a finer resolution (3.2-Hz bandwidth) narrow-band spectrum of the region of multiple pure tones seen in figure 16(a) for 120 percent of design speed. The multiple pure tone spikes, at the expected shaft rotation frequency spacing, are more than 10 decibels down from the blade passage tone level.

The SPL spectra at 130° from the fan inlet are presented in figure 17. One-third-octave spectra for 100 and 120 percent of fan design speed are given in figure 17(a) with corresponding narrow-band spectra in figure 17(b). It should be noted that the blade passing tone at design speed (fig. 17(a)) is split between two one-third-octave filters with no distinct tone noise peak. This tone spike is seen to exist as expected in the corresponding narrow-band spectrum of figure 17(b)). Data from both figures show a marked increase in both tone and broadband levels, indicating higher noise generation in the rear quadrant for 120 percent of fan design speed.

Directivity effects are presented in figure 18 which shows the overall SPL as a function of angle from fan inlet for selected fan speeds. These data are for the design area

nozzle. As the fan speed increases, the peak noise level is seen to shift from the front to the rear quadrant, with a marked rear quadrant dominance for speeds above design. Higher noise levels in the rear quadrant are commonly seen for noncutoff fans and imply that dominant noise generation in fan QF-9 occurs in the stator region.

Noise components. - As part of the one-third-octave analysis, an attempt was made to separate the tone and broadband components of the fan noise. Beginning with the total spectrum, an assumed broadband spectrum is drawn by disregarding those data points thought to be influenced by the tone noise. In many cases the tone spike was shared by two one-third-octave filters. The tone contribution to the SPL and PWL was found by performing a decibel subtraction of the assumed broadband spectrum level at each frequency from the data as shown in figure 19. All tone contributions, fundamental and harmonic, were then added to give the total tone level. Finally, this total tone value was subtracted from the overall for the spectrum to give the actual broadband SPL. Operation of the fan with a rotor relative Mach number appreciably greater than 1.0 would make this separation of tones much more difficult due to the prominant existence of multiple pure tones. For fan QF-9 this condition only occurred for the 120 percent of design speed data. Since MPT values were more than 10 decibels down, they were not separated into components. This method of separating the tone and broadband components is an approximation. A more exact approach is to work from fine resolution narrow band spectra. However, this greater resolution would also greatly increase the complexity of the calculations. Hence, the one-third-octave spectra were deemed sufficient for this study. A further discussion of the use of narrow band spectra for analyzing noise components is given in reference 20.

Using the tone and broadband separation method discussed with figure 19, the SPL directivity plot of figure 18 was separated into tone and broadband components in figure 20. The SPL tone component, figure 20(a), shows much more variation with fan speed in the rear quadrant than in the front quadrant. The over-design fan speed results are especially high in the rear quadrant. At 86 percent of design fan speed and above the tone SPL shows remarkably little variation with fan speed up to 60° from the fan inlet. Similar trends are noted for the broadband directivity with greater fan speed sensitivity observed in the rear quadrant (fig. 20(b)). However, the front quadrant broadband SPL increases in an expected manner with fan speed.

Sound power level. - The overall sound power level (OAPWL) is presented as a function of the stage pressure level in figure 21. At speeds below design (i.e., where the stage pressure ratio is less than 1.20) the results for the design and smaller nozzle areas are essentially the same. Opening the nozzle area to 5 percent over design added about 1 decibel to the OAPWL at any tested pressure ratio. Above design speed there is a marked difference in the results for the design and 92 percent of design area nozzle, with the design area nozzle showing the higher OAPWL at comparable pressure ratios. The increases in OAPWL above design speed in figure 21 may reflect the decrease in

aerodynamic performance of these test points for the design area nozzle resulting in more turbulent airflow.

The blade total loss coefficient gives an indication of the blade performance and has acoustic implications since higher loss coefficients are associated with worsening blade airflow conditions. The model fan results (refs. 3 and 4) include blade total loss coefficients. These results show a considerable increase in the total loss coefficient with a fan speed increase from design to 20 percent over design, thus providing aerodynamic rational for the higher noise associated with overspeed operation.

Another related aerodynamic parameter is the stage adiabatic efficiency. The efficiency results for the full-scale fan QF-9 stage likewise imply worsening flow conditions with operation above design speed. These efficiency results for fan QF-9 will be further discussed under the acoustic results section dealing with the effects of several rotor pitch angles.

The design-area nozzle OAPWL results of figure 21 were separated into tone and broadband components and plotted as functions of fan tip speed in figure 22. The OAPWL results are also given in this figure. The tone PWL component is seen to be a less significant part of the OAPWL at fan tip speeds above 200 meters per second, thus implying that broadband noise would control the overall noise.

Perceived noise levels. - The PNL's are frequency-weighted for human hearing, and, therefore, are of major importance in selecting a suitable fan for a STOL aircraft which is to operate near populated areas. The low number of rotor blades and relatively low rotor tip speed of fan QF-9 take advantage of this perceived noise weighting. Figure 23 is a noy curve showing the perceived noise spectrum for a 100-decibel SPL occurring at all frequencies. The perceived noisiness is highest at 3000 to 4000 hertz. The fan QF-9 fundamental first and second overtones are spotted on this noy spectrum and are seen to occur in a region of relatively low noy levels.

A perceived noise directivity plot for fan QF-9 with the design area nozzle is presented in figure 24. The perceived noise is calculated along a 152.4-meter (500-ft) sideline. Near the fan inlet the PNL shows little variation with fan speeds above 86 percent of design. However, past 50^{o} from the inlet the fan speed effect is quite evident, with the over-design speed results showing high rear quadrant PNL's. These high rear quadrant levels are even more pronounced than for the OAPWL directivity (fig. 18) and are controlled by the broadband noise component which is quite high in the region of maximum perceived noise sensitivity. In figure 24 the maximum calculated perceived noise along the 152.4-meter (500-ft) sideline at fan takeoff (design) speed was 100.1 PNdB.

The perceived noise directivity at design fan speed for the tested nozzle areas (fig. 25) shows only a slight but insignificant nozzle area effect in the rear quadrant, while the PNL in the front quadrant shows a more significant 4 decibel change. This relation between PNL and nozzle area is typical of that observed for other fans (e.g., see

refs. 13 and 14).

A history of the tone corrected perceived noise level (PNLT) for an aircraft flyover is presented in figure 26. The levels are calculated for four QF-9 fans operated at design speed and nozzle area each having a thrust level of 57 600 newtons (13 000 lbf). However, these results are not adjusted for core engine noise nor for possible aircraft aerodynamic noise or for forward motion effects. The aircraft is considered to fly overhead at a constant 152.4-meter (500-ft) altitude at a velocity of 41 meters per second (135 ft/sec). The peak flyover noise level occurs 2.5 to 3 seconds after the aircraft is directly overhead, indicating higher rear quadrant noise. Effective perceived noise level (EPNdB) is obtained by integrating the PNLT history with a standard normalization (ref. 21). For typical STOL aircraft flight profiles, a comparison of EPNdB and PNdB values shows that PNdB values are about 1 or 2 decibels higher than corresponding EPNdB results. For figure 26 the EPNdB level for four QF-9 fans is 105.2, which is considerably higher than the goal of 95 EPNdB. Hence, acoustic treatment would be required in conjunction with engines using the QF-9 fan to make it acceptable for use in a quiet STOL aircraft.

Noise predictions. - QF-9 fan data were used in reference 22 along with data from six other fans to develop a general fan noise prediction procedure. This procedure does not consider the jet noise contribution to the spectrum. A comparison of the predicted spectrum with QF-9 measured data at 40° and 120° is shown in figure 27. At 40° from the fan inlet (fig. 27(a)) the prediction is seen to approximate the broadband spectrum at most frequencies. However, the fundamental tone level is slightly overpredicted partly because the measured tone is shared between two one-third-octave filters. Noise contributions at frequencies below 200 hertz are associated with fan jet noise and are not included in the prediction. The correlation at 120° from the fan inlet (fig. 27(b)) using the method of reference 22 is also quite good, especially with respect to the fundamental blade passage and overtone levels. A prediction of the fan QF-9 PNL along a 152.4-meter (500-ft) sideline is compared to fan data in figure 27(c). The method of reference 22 gives results which compare within 2 decibels of the measured PNL at all angles; however, as noted, the QF-9 data were among the six inputs to the prediction method.

Approach Rotor Blade Pitch Angle

The fan QF-9 acoustic results for the designated approach rotor pitch angle (50°) will be presented in a manner similar to that used for the takeoff (64°) results. The designated approach fan speed for fan QF-9 is 86 percent of design, and the designated approach thrust is 36 000 newtons (8100 lbf), one-half of the takeoff (design) value.

Sound pressure level. - Representative front and rear quadrant approach rotor pitch SPL spectra are presented in figure 28. Results are shown for 86 and 100 percent of design fan speed. Front quadrant results at 20° from the fan inlet axis are given in figure 28(a). The spectra are typical with the only unexpected feature being the high blade passing tone level for 86 percent design fan speed at the front, 20° location. Even when the sharing of the passing tone between two one-third-octave filters for the design speed results of figure 28(a) is considered, the approach speed spectrum still has a slightly higher passing tone level. The 86 percent design fan speed SPL results exhibited a relatively high blade passing tone level at most measured front quadrant locations (see ref. 5). Rear quadrant results at 130° are in figure 28(b). The spectra are typical with both the fundamental blade passing tone and broadband increasing with speed.

The SPL directivity for the approach rotor angle and design nozzle area configuration is presented in figure 29 for five fan speeds. A few points at 150° and 160° from the fan inlet appear erratic and may have been influenced by the fan exhaust impinging the microphones. If these points are disregarded, fan QF-9 at approach has its highest SPL in the front quadrant at 30° or 40° from the fan inlet.

Sound power level. - The OAPWL at approach rotor angle is plotted as a function of the stage pressure ratio in figure 30. The nozzle area has considerable effect on the OAPWL at tested pressure ratios for the 50° rotor pitch angle. This contrasts with the slight nozzle area effect on the OAPWL at takeoff rotor angle (see fig. 21). At each tested pressure ratio, the OAPWL results for the 95 percent design area nozzle appear as a minimum.

The broadband and pure tone components of the SPL are plotted against corrected rotor tip speed in figure 31. Except for rotor tip speeds less than 150 meters per second, the tone and broadband components are essentially equal. In both figures 30 and 31 the acoustic data influenced by fan exhaust were modified by substituting adjacent microphone data which were free of exhaust effects.

Perceived noise. - The approach condition PNL along a 152.4-meter (500-ft) sideline for fan QF-9 is presented in figure 32. Results are shown for four nozzle areas. The maximum PNL is approximately the same in the front and rear quadrants for each nozzle area. While the largest nozzle area, 105 percent of design, resulted in the highest PNL, the trend of minimum noise at 95 percent design nozzle area noted in figure 30 was also the case for perceived noise.

Comparison of takeoff and approach conditions. - A plot of the maximum sideline PNL as a function of nozzle area is given in figure 33. Results are for the takeoff rotor angle at design fan speed and the approach rotor angle at 86 percent design fan speed. Changes in nozzle area resulted in very small PNL changes for the takeoff condition. However, the results for the approach condition showed considerable sensitivity to changes in nozzle area, again showing a minimum PNL for the 95 percent of design nozzle area.

Results for Several Rotor Pitch Angles

Several other forward-thrust rotor angle positions were tested in addition to takeoff (64^{o}) and approach (50^{o}) positions. In many cases minimum fan noise was found to occur at off-design rotor pitch angles. The relation of fan noise to the rotor pitch angle will be considered in this section in terms of PWL and PNL. Only results for the design area nozzle will be considered. The results of this section will be summarized in a map of stage thrust as a function of fan speed with superimposed lines of maximum sideline PNL.

A further discussion of the relation of noise to rotor pitch angle for the fan is available in reference 23. The reference further establishes the role of the rotor loss coefficient as it relates to fan noise generation with conditions of minimum fan noise corresponding to minimum rotor loss coefficient.

Sound power level. - Reference 24 develops a method whereby noise results may be normalized with respect to thrust by subtracting 10 $\log_{10}$ (thrust) from the noise values. This procedure was applied to the OAPWL results and these adjusted results are plotted as functions of rotor pitch angle in figure 34. On this basis, a rotor pitch angle of 57^{o} appears to produce the least noise.

Perceived noise. - The maximum PNL for several stage thrust values are presented as a function of rotor pitch angle in figure 35. At constant thrust, the minimum sideline PNL is seen to shift with increasing thrust. At approach, which has a thrust level of one-half the stage design thrust, the minimum sideline PNL occurs at a rotor pitch angle of 57^{o}. This minimum noise rotor pitch angle shifts to the design value of 64^{o} for thrust levels approaching design. This relation of thrust and noise is summarized in the plot of corrected thrust as a function of fan speed in figure 36. Lines of constant sideline PNL are superimposed on the aerodynamic results.

Reference 9 comments that predicted maximum stage efficiency occurs at points of minimum fan noise. The fan QF-9 efficiency results are consistent with the conclusions as may be seen from the plot of stage adiabatic efficiency as a function of rotor pitch angle (fig. 37). Because of the uncertainty in the magnitudes of the measured efficiencies for the full-scale fan (as discussed in the Aerodynamic Performance section) the results of figure 37 are plotted on a relative scale of efficiency points. The trends of the efficiency levels as a function of rotor pitch angle are generally the inverse of the noise behavior. The maximum efficiency occurs for a rotor pitch angle of 57^{o} to 64^{o} generally following the fan speed relation for minimum noise noted for figure 36. Overspeed results, which show increased noise levels, show a reduced stage efficiency.

Reverse Thrust Rotor Pitch Angle

One of the major features of the fan QF-9 design is the ability to adjust the rotor blade pitch angle to achieve thrust reversal. The fan QF-9 rotor blade passes through feather position to the reverse thrust setting or 148° (fig. 6). A blast deflector was erected between the drive motor building and the fan stage (see fig. 8(b)) to protect the drive motor building wall from possible wind damage during reverse thrust tests. For reverse thrust tests, a nozzle with divergent walls was used as the inlet to simulate a bellmouth. A similar arrangement would be required on an engine application of a reversing fan such as QF-9. Results for the scale model fan run in the reverse thrust configuration are available in reference 25.

Sound pressure level. - Fan QF-9 was run in the reverse thrust mode both with and without the blast deflector to determine the effect this deflector would have on noise measurements. This comparison is presented in the SPL spectra of figure 38 for design fan speed. Figure 38(a) presents one-third-octave spectra at 150° from the normal fan inlet axis (drive shaft end), which is temporarily the inlet in the reverse thrust mode. The spectral differences at blade passing frequency are due to slight fan speed differences which resulted in a different one-third-octave reduction of this passing tone. Different ambient temperatures for the two tests necessitated these fan speed differences to maintain the desired corrected fan speed. Figure 38(b) presents spectra at 40° from the fan inlet. Narrow-band SPL spectra corresponding to the one-third-octave results of figure 38 are presented in figure 39 for the reverse thrust configuration with the blast deflector installed. It is evident that the blast deflector had little influence on the acoustic results.

Sound power level. - Figure 40 compares the PWL spectra for fan QF-9 for forward and reverse thrust configurations at design fan speed. The forward thrust results are for the takeoff (64°) rotor angle and design nozzle area. Reverse thrust mode PWL results are higher than corresponding forward thrust results. This is true for both broadband and blade passage tone levels. In addition, reverse thrust operation generates a significant facility related broadband noise contribution which peaks around 160 hertz and arises from the high-speed exhaust flow scrubbing over the fan drive shaft and supports during reverse thrust operation.

The PWL was separated into broadband and tone components, and they were plotted as functions of corrected rotor tip speed in figure 41. At all tested fan speeds the broadband noise was the major component of the PWL as might be expected from the interaction of the rotor with the stator wakes for reverse thrust flow conditions.

Perceived noise. - In reverse thrust operation the PNL along a 152.4-meter (500-ft) sideline is highest in the front quadrant as shown in the directivity plot of figure 42. The PNL tended to be highest in the rear quadrant for forward thrust operation of fan QF-9 (see figs. 25 and 32). In short, the highest PNL is always observed in the exhaust quad-

rant regardless of flow direction.

Figure 43 presents the maximum PNL along a 152.4-meter (500-ft) sideline as a function of percent of fan design speed. The design takeoff rotor angle, nozzle area, and fan speed results are compared to the reverse thrust results at comparable fan speeds on this figure. The reverse thrust PNL are about 4 to 5 PNdB above takeoff results at comparable fan speeds.

SUMMARY OF RESULTS

This report presents the acoustic and aerodynamic performance for a 1.83-meter-(6-ft-) diameter experimental fan stage with characteristics suitable for a low-noise STOL engine. The 1.2 pressure ratio fan stage, designated QF-9, incorporated features for low noise including the elimination of inlet guide vanes, low rotor blade tip speed, long axial spacing between the rotor and stator blade rows, and low number of rotor blades. The QF-9 fan featured adjustable pitch rotor blades which were incorporated primarily for thrust reversal but also as a way to optimize thrust noise relations for forward thrust operation.

The QF-9 was run without acoustic suppression in the flow passages. Four nozzle areas were tested. Tests were made in the speed range from 60 to 120 percent of fan takeoff (design) value.

Summary of Aerodynamic Results

The measured values of mass flow and stage pressure ratio fell somewhat short of the design-predicted values. At takeoff (64^{o}) rotor pitch angle the measured inlet corrected mass flow was approximately 4 percent low and the stage pressure ratio was 1.17 as compared to the predicted 1.20. The maximum stage pressure ratio of 1.265 was obtained at 120 percent of design fan speed with a nozzle area 92 percent of design.

At approach (50^{o}) rotor pitch angle the measured inlet corrected mass flow was approximately $3\frac{1}{2}$ percent low and the stage pressure ratio was 1.08 as compared to the predicted 1.096. The maximum stage pressure ratio of 1.129 was reached at 100 percent of takeoff speed with the nozzle having 92 percent of design area.

Adjusting the fan rotor blades to a pitch angle of 69^{o} increased both pressure ratio and mass flow. The measured stage pressure ratio at takeoff (design) fan speed (rotor tip speed, 213 m/sec) and design nozzle area was 1.188, slightly below design. The measured inlet corrected mass flow was 403 kilograms per second (888 lbm/sec), essentially the design value.

Forward thrust data from a range of nozzle sizes, rotor angles, and fan speeds in-

dicate that aerodynamic performance goals could be approached by either an increase in fan design speed or resetting the fan pitch angle to 69^{o} and decreasing the fan exhaust nozzle area to 92 percent of design nozzle area.

When compared to forward thrust, the measured inlet corrected mass flow for reverse thrust at design fan speed was about 65 percent of the flow measured at takeoff design conditions.

Summary of Acoustic Results

The acoustic results for fan QF-9 were presented for several forward thrust rotor pitch angles, including the takeoff (design) angle of 64^{o} and the designated approach angle of 50^{o}. Also, results were given for the reverse thrust configuration with a rotor pitch angle of 148^{o}.

Some of the significant results of these investigations are as follows:

1. The maximum perceived noise along the 152.4-meter (500-ft) sideline for takeoff design configuration was 100.1 PNdB. However, the EPNdB flyover noise level calculated from the static measurements for an aircraft employing four QF-9 fans was 105.2 decibels at 152.4 meters (500 ft). Hence, acoustic treatment would be required to meet present guidelines for use in a quiet STOL aircraft.

2. For takeoff, thrust, and with the design area nozzle, the minimum sideline PNL occurred at a rotor pitch angle of 64^{o}, the design value. However, for approach thrust level (one-half the takeoff thrust) the minimum sideline PNL occurred at a rotor pitch angle of 57^{o}.

3. The fan stage adiabatic efficiency generally showed a maximum value for minimum noise run conditions. Likewise, the scale model QF-9 fan rotor loss coefficient results minimized for operating conditions corresponding to those producing minimum noise in the full-scale fan.

4. For the design configuration, the perceived noise was highest in the aft quadrant with the most PNL variation with fan speed likewise observed in the aft quadrant.

5. The one-third-octave spectra were used to separate the broadband and pure tone components of the fan noise. The broadband components of SPL were seen to be the more significant part of the OAPNL at fan tip speeds above 198 meters per second (651 ft/sec), thus implying that broadband noise would control the overall noise.

6. Reverse thrust operation resulted in PNL's 4 to 5 PNdB above takeoff levels at comparable fan speeds. The noise peaked in the front quadrant (the exhaust quadrant for reverse thrust operation). The SPL spectra for reverse thrust operation showed the noise increase to include a significant jet noise contribution in addition to increased higher frequency broadband noise relative to the forward thrust design configuration results.

7. The maximum sideline PNL was considerably more sensitive to nozzle area effects at the approach rotor pitch angle than for the takeoff pitch angle. For example, the maximum sideline PNL was nearly constant over the range of tested nozzle areas for the takeoff rotor pitch angle and design fan speed. However, a clear minimum was evident in about 6 PNdB variation over the nozzle area range tested at the approach rotor pitch angle and the designated 86 percent design approach fan speed.

Lewis Research Center,
National Aeronautics and Space Administration,
Cleveland, Ohio, August 26, 1976,
505-03.

APPENDIX - AERODYNAMIC CALCULATIONS

Symbols

A	flow area, m^2
a	speed of sound at standard conditions, m/sec
CF	bellmouth flow coefficient
F	thrust, N
g	gravitational constant
M	Mach number
P	total pressure, gage, N/m^2
P_0	ambient total pressure, N/m^2
PR	pressure ratio
R	universal gas constant
S	static pressure, gage, N/m^2
T	total temperature, K
T_0	ambient temperature, K
TR	temperature ratio
V	velocity, m/sec
W	mass flow, kg/sec
γ	ratio of specific heats, 1.4 used for air
δ	ratio of total pressure to standard pressure
η	adiabatic temperature rise efficiency
θ	ratio of total temperature to standard temperature

Subcripts:

C	corrected
T	total
0	ambient
1	inlet duct static measuring station
3	stator discharge measuring station
5	nozzle discharge measuring station

9 bellmouth lip measuring station

Equations

Total temperature:

$$T = \frac{\sum_{1}^{6} T_9}{6}$$

Inlet duct static pressure:

$$S_1 = \frac{\sum_{1}^{6} S_1}{6}$$

Inlet duct Mach number:

$$M_1 = \sqrt{\frac{\left(\frac{P_0}{P_0 + S_1}\right)^{2/7} - 1}{0.2}}$$

Corrected inlet mass flow:

$$W_{C1} = \frac{\frac{101\ 325\ N/m^2}{288.15\ K}\sqrt{\frac{\gamma g}{R}} \cdot A_1 \cdot M_1 \cdot CF}{\left(1 + 0.2\ M_1^2\right)^3}$$

where standard atmosphere is 101 325 N/m^2 (14.70 psi) and standard temperature is 288.15 K (15° C, 59° F).

Total inlet mass flow:

$$W_{T1} = W_{C1} \frac{\delta_1}{\sqrt{\theta_1}}$$

where

$$\delta_1 = \frac{P_0}{101\ 325\ N/m^2}$$

$$\theta_1 = \frac{T_0 + 273.15\ K}{288.15\ K}$$

Stator discharge Mach number:

$$M_3(a) = \sqrt{\frac{\left[\frac{P_3(a) + P_0}{S_3(a) + P_0}\right]^{2/7} - 1}{0.2}}$$

Corrected stator exit mass flow:

$$W_{C3}(a) = \frac{\frac{101\ 325\ N/m^2}{\sqrt{288.1\ K}} \sqrt{\frac{\gamma g}{R}}\ \sqrt{5}\ A_3(a) \sqrt{\frac{P_3(a) + P_0}{S_3(a) + P_0} - 1}}{\left[\frac{P_3(a) + P_0}{S_3(a) + P_0}\right]^{6/7}}$$

where $A_3(a)$ is the flow area associated with each rake total pressure element, and for n rake elements

$$W_{C3} = \sum W_{C3}(a)$$

Total stator exit mass flow:

$$W_{T3}(a) = W_{C3} \frac{\delta_3(a)}{\sqrt{\theta_3(a)}}$$

where

$$\delta_3(a) = \frac{P_3(a) + P_0}{101\ 325\ N/m^2}$$

$$\theta_3(a) = \frac{T_3(a) + 273.15\ K}{288.15\ K}$$

for each rake total pressure element a.

$$W_{T3} = \sum_{a=1}^{n} W_{T3}(a)$$

Stage pressure ratio:

$$PR = \frac{\dfrac{\sum_{a=1}^{n} [P_3(a) + P_0]}{P_0} \cdot W_{T3}(a)}{W_{T3}}$$

Stage temperature ratio:

$$TR = \frac{\sum_{a=1}^{n} [T_3(a) + 273.15] \cdot W_{T3}(a)}{W_{T3} \cdot (T + 273.15)}$$

Stage adiabatic efficiency:

$$\eta = \frac{PR^{2/7} - 1}{TR - 1}$$

Nozzle discharge Mach number (calculated at each discharge rake element location c):

$$M_5(c) = \sqrt{\frac{\left[\frac{P_5(c) + P_0}{S_5(c) + P_0}\right]^{2/7} - 1}{0.2}}$$

Local exhaust velocity:

$$V_5(c) = \frac{M_5(c) \cdot a \cdot \sqrt{\theta_5}}{1 + 0.2[M_5(c)]^2}$$

where

$$\sqrt{\theta_5} = \sum_{a=1}^{n} \sqrt{\theta_3(a)} \cdot \frac{W_{C3}(a)}{W_{T3}}$$

Stage thrust:

$$F_5(c) = \frac{1.4\ M_5(c) \cdot A_5(c) \cdot [P_5(c) + P_0]}{\left\{1 + 0.2[M_5(c)]^2\right\}^{7/2}} + [A_5(c) \cdot S(c)]$$

where $A_5(c)$ is the flow area associated with each rake total pressure element, and for n rake elements

$$F_5 = \sum_{c=1}^{n} F_5(c)$$

Corrected stage thrust:

$$F_{C5} = \frac{F_5}{\delta_1}$$

REFERENCES

1. Rulis, Raymond J.: STOL Noise Sources and Fan Noise Treatment. Aircraft Engine Noise Reduction. NASA SP-311, 1972, pp. 247-258.

2. Rulis, R. J.: Status of Current Development Activity Related to STOL Propulsion Noise Reduction. SAE Paper 730377, Apr. 1973.

3. Lewis, George W., Jr.; and Tysl, Edward R.: Overall and Blade-Element Performance of a 1.20 Pressure-Ratio Fan Stage at Design Blade Setting Angle. NASA TM X-3101, 1974.

4. Lewis, George W., Jr.; Moore, Royce D.; and Kovich, George: Performance of a 1.20-Pressure-Ratio STOL Fan Stage at Three Rotor Blade Setting Angles. NASA TM X-2837, 1973.

5. Glaser, Frederick W.; Wazyniak, Joseph A.; and Friedman, Robert: Noise Data from Tests of a 1.83-Meter (6-ft) Diameter Variable-Pitch 1.2 Pressure-Ratio Fan (QF-9). NASA TM X-3187, 1975.

6. Source Abatement Technology. Aircraft Noise Reduction Technology. Sec. III, NASA TM X-68241, 1973, pp. 13-112.

7. Crigler, John L.; and Copeland, W. Latham: Noise Studies of Inlet-Guide-Vane - Rotor Interaction of a Single-Stage Axial-Flow Compressor. NASA TN D-2962, 1965.

8. Dittmar, James H.: Methods for Reducing Blade Passing Frequency Noise Generated by Rotor-Wake-Stator Interaction. NASA TM X-2669, 1972.

9. Metzger, F. B.: Progress in Source Noise Suppression of Subsonic Tip Speed Fans. AIAA Paper 73-1032, Oct. 1973.

10. Lowson, M. V.: Reduction of Compressor Noise Radiation. J. Acous. Soc. Am., vol. 43, no. 1, Jan. 1968, pp. 37-50.

11. Tyler, J. M.; and Sofrin, T. G.: Axial Flow Compressor Noise Studies. SAE Trans., vol. 70, 1962, pp. 309-332.

12. Sofrin, T. G.; and Pickett, G. F.: Multiple Pure Tone Noise Generated by Fans at Supersonic Tip Speeds. International Symposium on the Fluid Mechanics and Design of Turbomachinery. Pennsylvania State University, 1970, pp. 435-459.

13. Woodward, Richard P.; Lucas, James G.; and Stakolich, Edward G.: Acoustic and Aerodynamic Performance of a 1.83 Meter (6 ft) Diameter 1.2 Pressure Ratio Fan (QF-6). NASA TN D-7809, 1974.

14. Woodward, Richard P.; and Lucas, James G.: Acoustic and Aerodynamic Performance of a 1.83 Meter (6-ft) Diameter 1.25 Pressure Ratio Fan (QF-8). NASA TN D-8130, 1976.

15. Sagerser, David A.; Schaefer, John W.; and Dietrich, Donald A.: Reverse Thrust Technology for Variable Pitch Fan Propulsion Systems. Powered-Lift Aeronautics and Acoustics, NASA SP-406, 1976.

16. Leonard, Bruce R.; et al.: Acoustic and Aerodynamic Performance of 6-Foot Diameter Fans for Turbofan Engines. Part I - Design of Facility and QF-1 Fan. NASA TN D-5877, 1970.

17. Standard Values of Atmospheric Absorption as a Function of Temperature and Humidity for Use in Evaluating Aircraft Flyover Noise. Aerospace Recommended Practice No. 866, SAE, Aug. 1964.

18. Montegani, Francis J.: Some Propulsion System Noise Data Handling Conventions and Computer Programs Used at the Lewis Research Center. NASA TM X-3013, 1974.

19. Definitions and Procedures for Computing Perceived Noise Levels of Aircraft Noise. Aerospace Recommended Practice No. 865A, SAE, Aug. 1969.

20. Saule, Arthur V.: Some Observations About the Components of Transonic Fan Noise from Narrow-Band Spectral Analysis. NASA TN D-7788, 1974.

21. Noise Standards, Aircraft Type and Airworthiness Certification. Federal Aviation Regulations, pt. 36, June 1974.

22. Heidmann, Marcus F.: Interim Prediction Method for Fan and Compressor Source Noise. NASA TM X-71763, 1975.

23. Woodward, Richard P.; and Glaser, Frederick W.: Acoustic and Aerodynamic Effects of Rotor Pitch Angle for a Variable Pitch, 6-Foot-Diameter Fan Stage. AIAA Paper 76-573, July 1976.

24. Heidmann, M. F.; and Feiler, C. E.: Noise Comparisons from Full-Scale Fan Tests at NASA Lewis Research Center. AIAA Paper 73-1017, Oct. 1973.

25. Moore, Royce D.; Lewis, George W., Jr.; and Tysl, Edward R.: Performance of a Low-Pressure Fan Stage With Reverse Flow. NASA TM X-3349, 1976.

TABLE I. - AERODYNAMIC DESIGN PARAMETERS

Overall total pressure ratio	1.20
Corrected rotor tip speed, m/sec (ft/sec)	213.3 (700)
Predicted overall efficiency, percent	90.2
Corrected inlet weight flow, kg/sec (lb/sec)	403 (889)
Corrected inlet specific weight flow, kg/sec-m^2 (lb/sec-ft^2)	194.8 (39.9)
Stage thrust, N (lb)	71 705 (16 120)
Work coefficient	0.369
Rotor head-rise coefficient	0.348
Stage head-rise coefficient	0.334
Rotor tip diameter, m (ft)	1.829 (6.0)

TABLE II. - BLADE DESIGN PARAMETERS

	Rotor	Stator
Number of blades	15	11
Chord, cm (in.)		
Hub	21.5 (8.46)	38.1 (15.0)
Tip	34.3 (13.5)	38.1 (15.0)
Solidity		
Hub	1.219	1.406
Tip	0.893	0.714
D-factor		
Hub	0.530	0.512
Maximum	0.530	0.512
Tip	0.431	0.363
Camber angle, deg		
Hub	44.89	52.50
Tip	18.40	56.40
Chord angle, deg, relative to fan axis		
Hub	5.61	16.30
Tip	41.14	11.32
Mean aspect ratio	1.70	1.23
Rotor inlet hub-tip radius ratio	0.460	-----
Tip relative inlet Mach number	0.865	-----
Material	Composite and titanium	Aluminum
Corrected speed, rpm	2227.0	-----
Blade passage frequency, Hz	557	-----
Mean rotor-stator separation, rotor chords	2	-----

TABLE III. - TEST CONFIGURATIONS

Configuration description		Comments
Rotor blade pitch angle, B_R, deg	Nozzle area, percent of design[a]	
64 (takeoff)	100 95 92 105	Far-field noise
50 (approach)	100 95 92 105	Far-field noise
57 69 45	100 100 100	Far-field noise
59 64 64	100 100 92	Far-field noise, overspeed
148 (reverse)	105	Far-field noise

[a]Design nozzle area, 2.02 m^2 (21.75 ft^2).

TABLE IV. - SELECTED AERODYNAMIC RESULTS

Configuration description		Percent of design speed	Corrected, rpm	Corrected tip speed		Inlet duct Mach number	Stage pressure ratio	Corrected inlet weight flow		Corrected thrust	
Rotor blade pitch angle, B_R, deg	Nozzle area, percent of takeoff			m/sec	ft/sec			kg/sec	lb/sec	N	lb
64 (takeoff)	100	60	1328	128	421	0.223	1.060	238	525	21 300	4 790
		70	1550	149	490	.262	1.081	276	608	28 600	6 440
		86	1898	183	601	.327	1.125	336	742	42 900	9 650
		93	2059	198	651	.357	1.146	363	800	49 600	11 200
		100	2214	213	700	.386	1.170	388	855	57 600	13 000
	95	60	1338	128	421	0.212	1.061	226	498	20 700	4 660
		70	1554	149	490	.249	1.084	263	580	28 000	6 300
		86	1905	183	601	.310	1.128	321	708	42 100	9 470
		93	2068	198	651	.340	1.152	349	769	50 400	11 300
		100	2222	213	700	.367	1.175	372	820	56 900	12 800
	92	60	1328	128	421	0.202	1.064	216	476	20 700	4 640
		70	1546	149	491	.237	1.087	251	554	28 000	6 300
		86	1893	183	601	.297	1.133	308	680	42 100	9 460
		93	2051	198	651	.323	1.157	333	734	49 400	11 000
		100	2210	214	702	.352	1.185	358	790	57 500	12 900
	105	60	1335	128	421	0.233	1.059	248	546	22 000	4 940
		70	1557	149	491	.274	1.080	287	634	30 200	6 790
		86	1904	183	601	.342	1.123	349	770	44 200	9 930
		93	2068	198	651	.371	1.144	375	827	51 200	11 500
		100	2220	213	700	.400	1.166	400	881	58 700	13 200
50 (approach)	100	60	1343	128	420	0.182	1.040	195	431	14 300	3 220
		70	1567	149	490	.211	1.054	225	497	19 400	4 360
		86	1920	183	601	.760	1.080	274	604	28 800	6 480
		93	----	---	---	-----	-----	---	---	------	------
		100	2238	213	700	.302	1.107	313	691	38 500	8 660
	95	60	1308	128	420	0.177	1.043	190	419	14 800	3 320
		70	1526	149	490	.205	1.058	220	484	19 800	4 450
		86	1868	183	601	.252	1.087	266	586	28 900	6 500
		93	2026	198	651	.273	1.101	287	633	33 800	7 590
		100	2178	213	700	.294	1.117	307	676	39 200	8 810
	92	60	1312	128	420	0.169	1.045	182	402	14 500	3 270
		70	1531	149	490	.201	1.063	215	473	20 400	4 600
		86	1874	183	601	.246	1.094	260	574	30 400	6 840
		93	2036	199	653	.769	1.112	282	622	35 300	7 940
		100	2186	214	701	.290	1.129	303	667	40 900	9 190
	105	60	1304	128	420	0.189	1.039	203	448	13 500	3 030
		70	1519	149	490	.220	1.051	235	518	18 800	4 220
		86	1858	182	599	.268	1.078	282	622	28 400	6 390
		93	2018	198	651	.291	1.090	303	669	33 400	7 510
		100	2168	213	700	.311	1.104	322	711	38 800	8 730

57	100	60	1327	129	422	0.203	1.050	217	479	17 800	4 010
		70	1546	150	492	.239	1.068	253	558	24 400	5 490
		86	1894	183	602	.295	1.101	308	678	36 300	8 150
		93	----	---	----	-----	-----	---	---	------	------
		100	2204	214	701	.347	1.136	354	780	47 800	10 800
69	100	60	1314	128	421	0.234	1.066	248	547	24 500	5 510
		70	1533	149	491	.276	1.091	290	639	33 100	7 440
		86	1878	183	601	.345	1.140	352	777	48 700	10 900
		93	2037	199	652	.378	1.165	381	839	57 400	12 900
		100	2190	214	702	.404	1.188	403	888	65 700	14 800
45	100	60	1324	128	421	0.171	1.035	184	406	13 000	2 930
		70	1545	149	491	.198	1.047	212	468	17 400	3 920
		86	1890	183	601	.241	1.069	255	563	25 300	5 680
		93	2051	199	652	.260	1.080	274	604	29 500	6 640
		100	2205	213	700	.279	1.091	292	644	33 800	7 590
59	100	100	2159	214	701	0.368	1.155	373	822	52 700	11 800
		110	2369	235	770	.407	1.185	403	888	62 900	14 100
		115	2475	245	806	.416	1.196	412	908	64 700	14 600
		120	2586	256	840	.424	1.202	419	923	67 500	15 200
64 (takeoff)	100	100	2163	213	700	0.395	1.177	395	871	60 300	13 600
		110	2382	235	770	.431	1.210	424	935	68 800	15 500
		115	2489	245	806	.440	1.222	431	950	71 900	16 200
		120	2596	256	840	.446	1.231	435	959	73 600	16 500
	92	100	2162	213	700	0.348	1.180	355	783	58 300	13 100
		110	2385	235	770	.390	1.224	391	861	68 800	15 500
		115	2486	245	806	.409	1.246	407	897	74 400	16 700
		120	2599	256	840	.425	1.265	419	923	79 300	17 800
148 (reverse)	105	86	1935	183	601	0.269	-----	223	492	------	------
		93	2100	198	651	.291	-----	239	527	------	------
		100	2257	213	700	.311	-----	254	559	------	------

Figure 1. - View of QF-9 rotor blading.

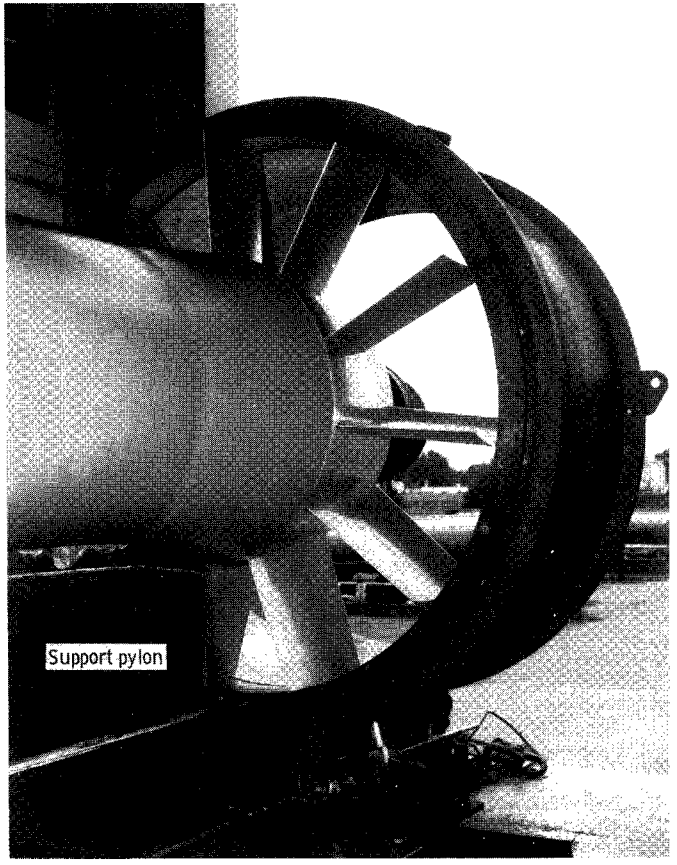

Figure 2. - View of QF-9 stator blading.

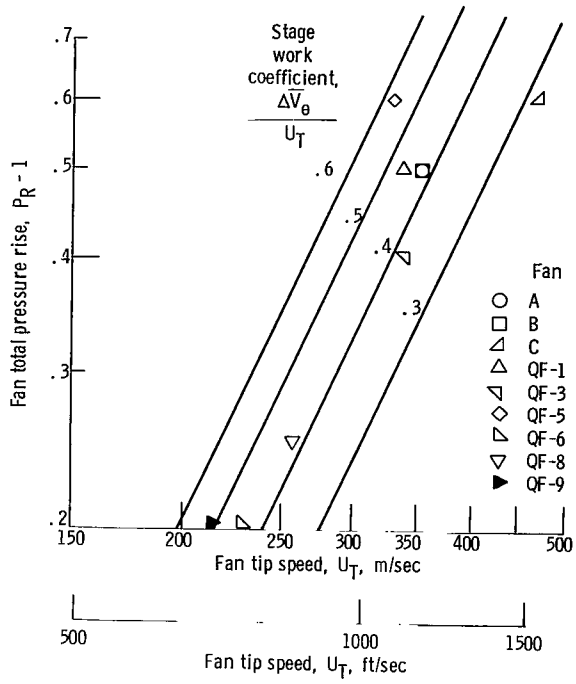

Figure 3. - Matrix of design parameters for fans tested at Lewis quiet fan facility.

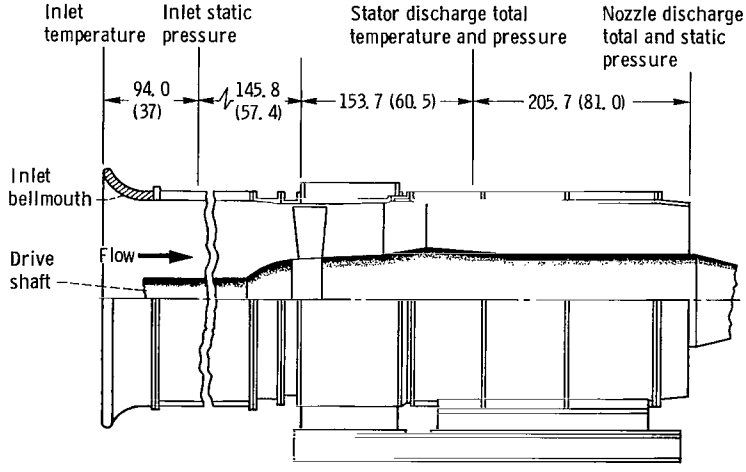

Figure 4. - Forward thrust configuration of QF-9 stage showing axial location of instrumentation. (All dimensions given in cm (in.).)

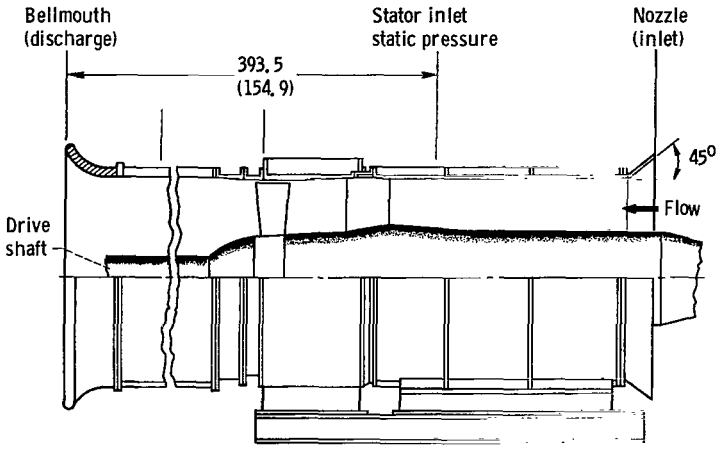

Figure 5. - Reverse thrust configuration of QF-9 stage showing axial location of instrumentation. (All dimensions given in cm (in.).)

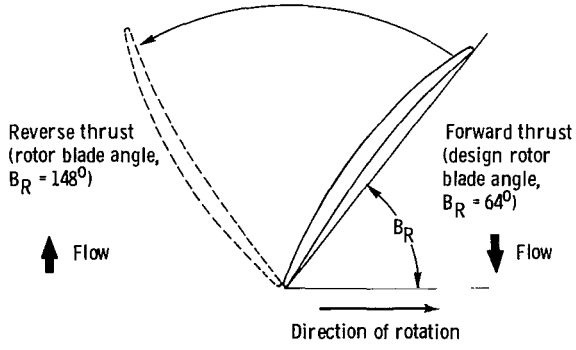

Figure 6. - Rotor pitch angle geometry. Blade passes through feather to reverse thrust position.

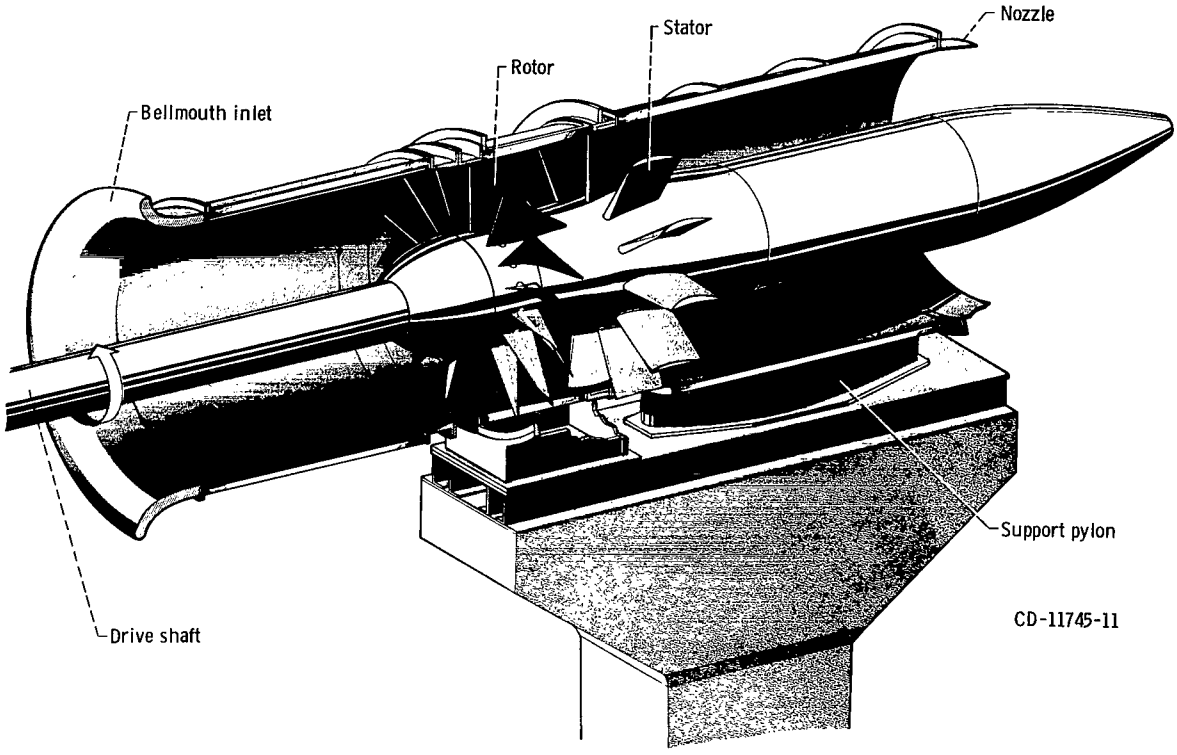

Figure 7. - Cutaway sketch of QF-9 fan installation.

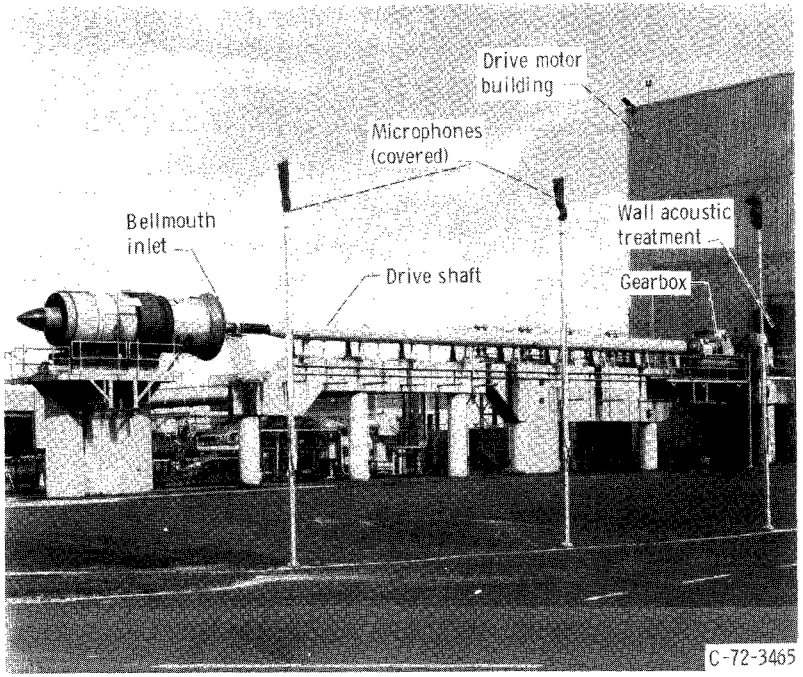

(a) Takeoff configuration.

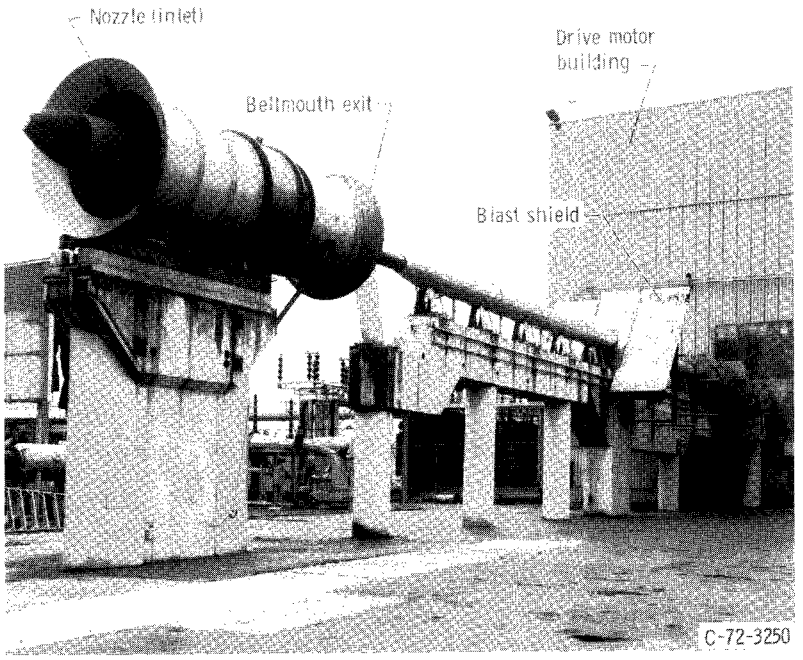

(b) Reverse thrust configuration.

Figure 8. - Test site showing QF-9 in place.

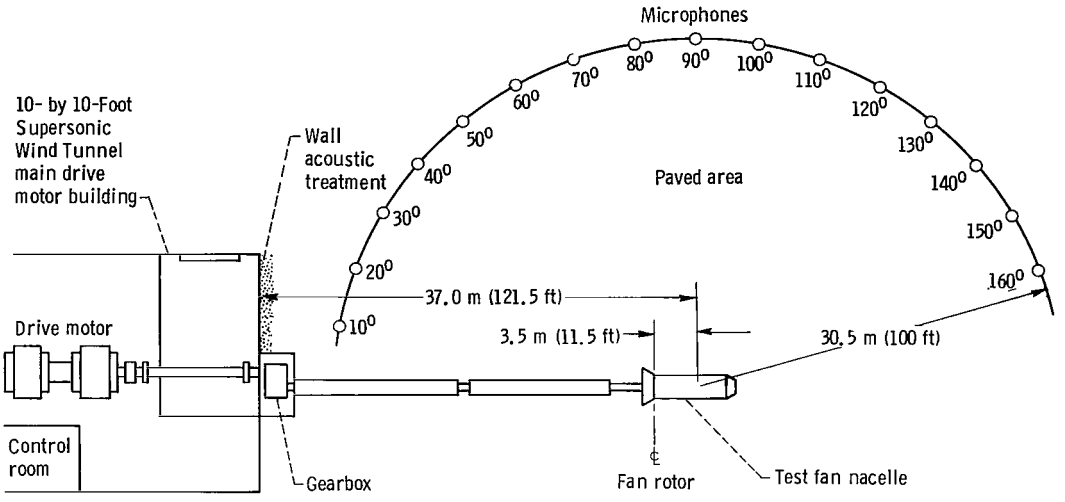

Figure 9. - Plan view of test site. (All dimensions given in m (ft).)

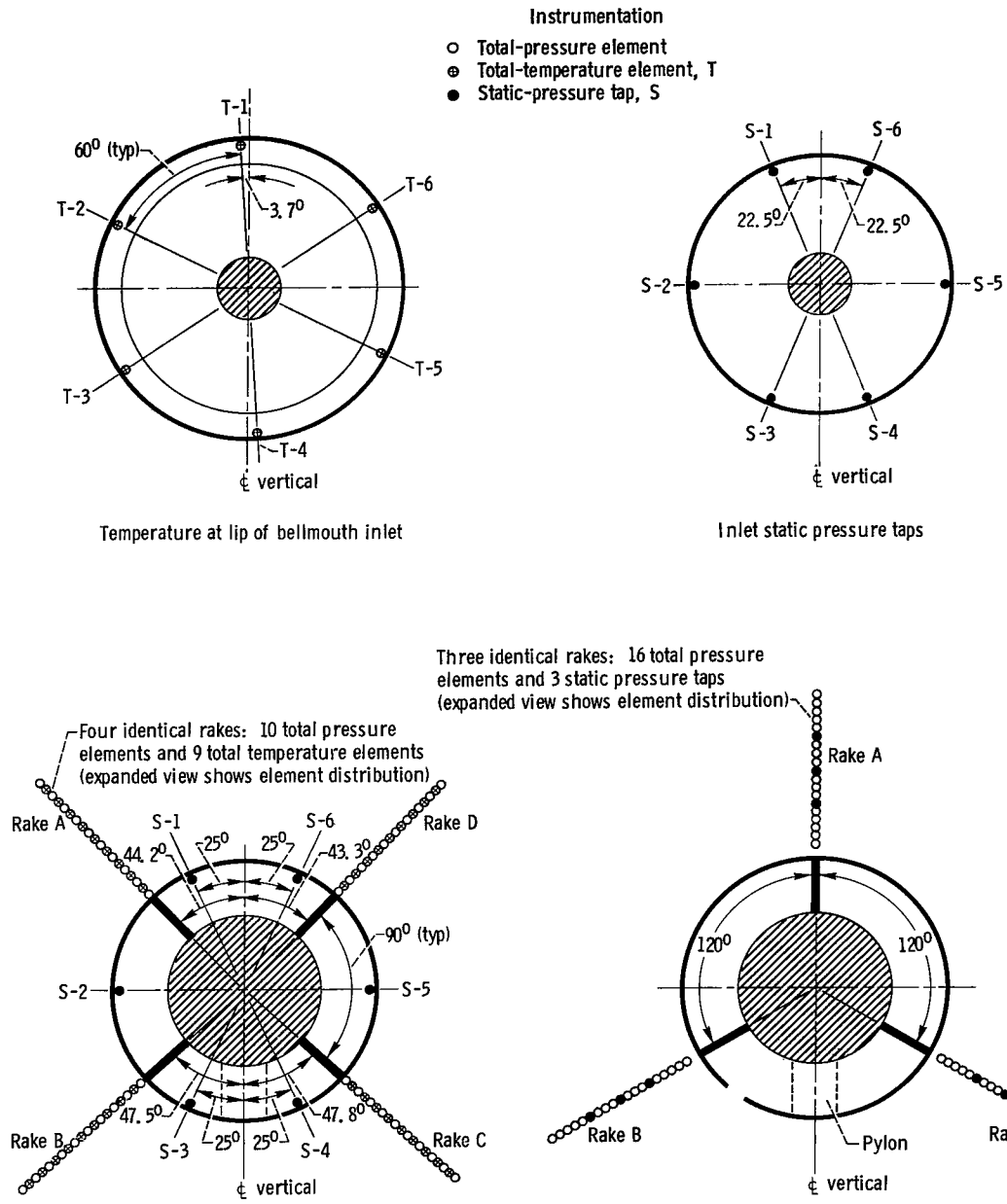

Figure 10. - Detail of fan aerodynamic instrumentation. All views looking downstream.

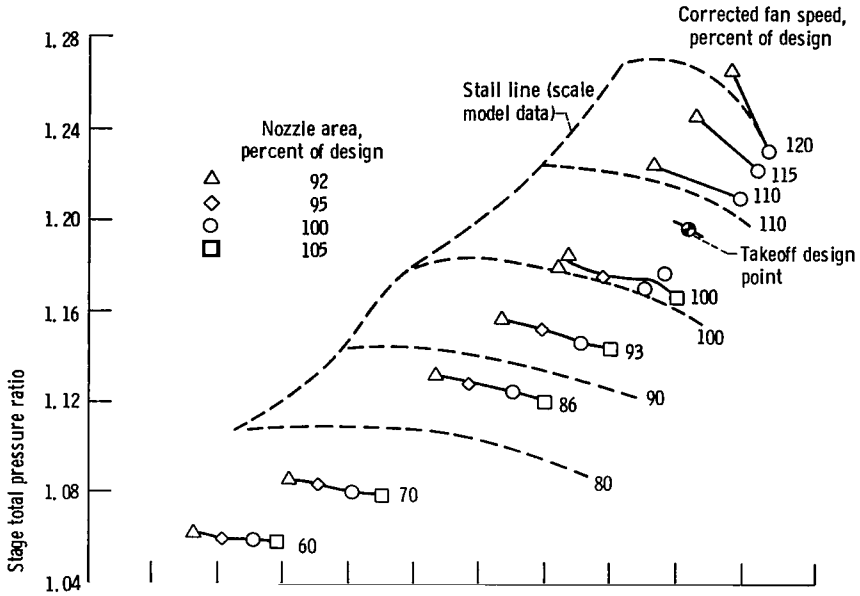

(a) Rotor blade at takeoff angle, 64^{0}.

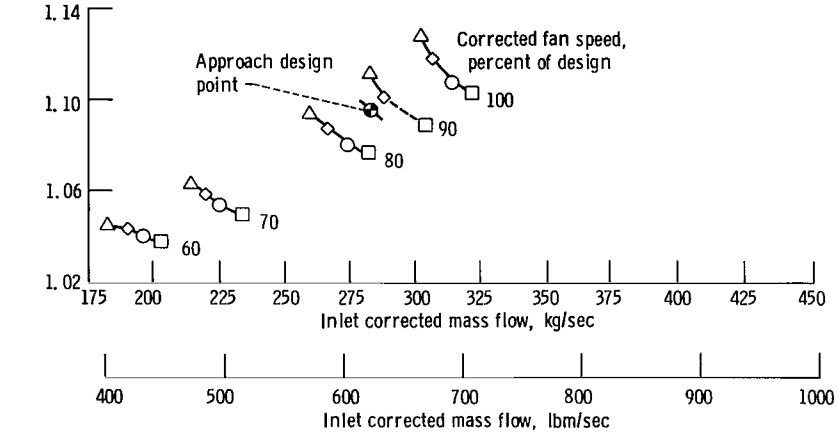

(b) Rotor blade at approach angle, 50^{0}.

Figure 11. - Fan operating map.

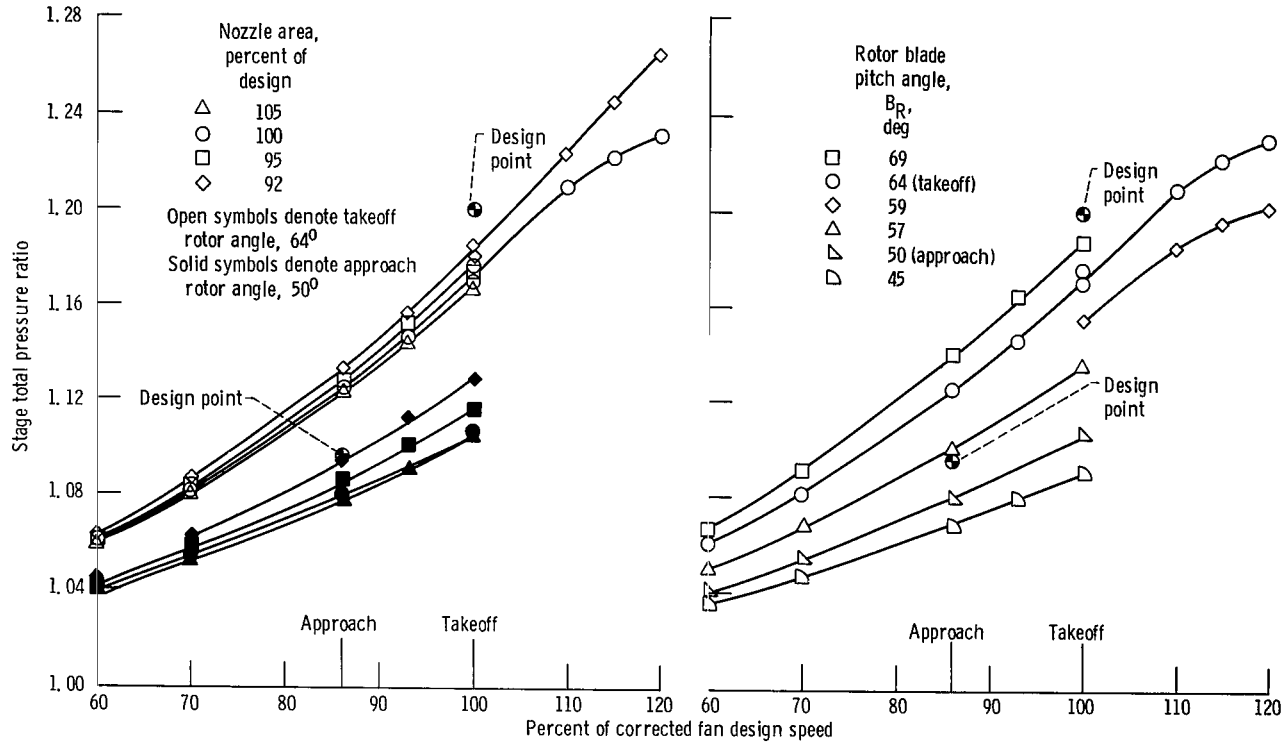

(a) For two rotor blade pitch angles and four nozzle area.

(b) For six rotor blade pitch angles at design nozzle area.

Figure 12. - Stage total pressure ratio as function of percent of corrected fan design speed.

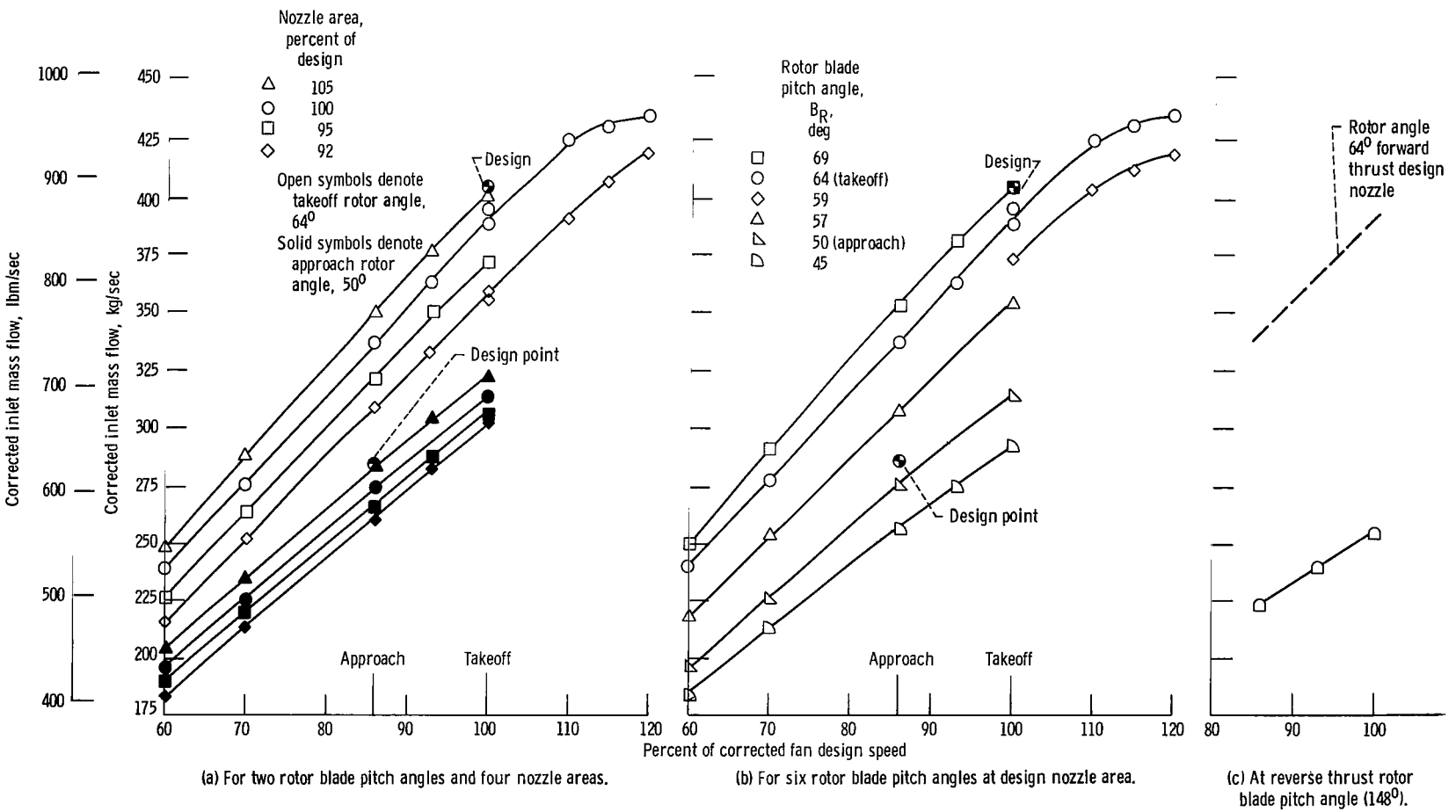

Figure 13. - Corrected inlet mass flow as function of percent of corrected fan design speed.

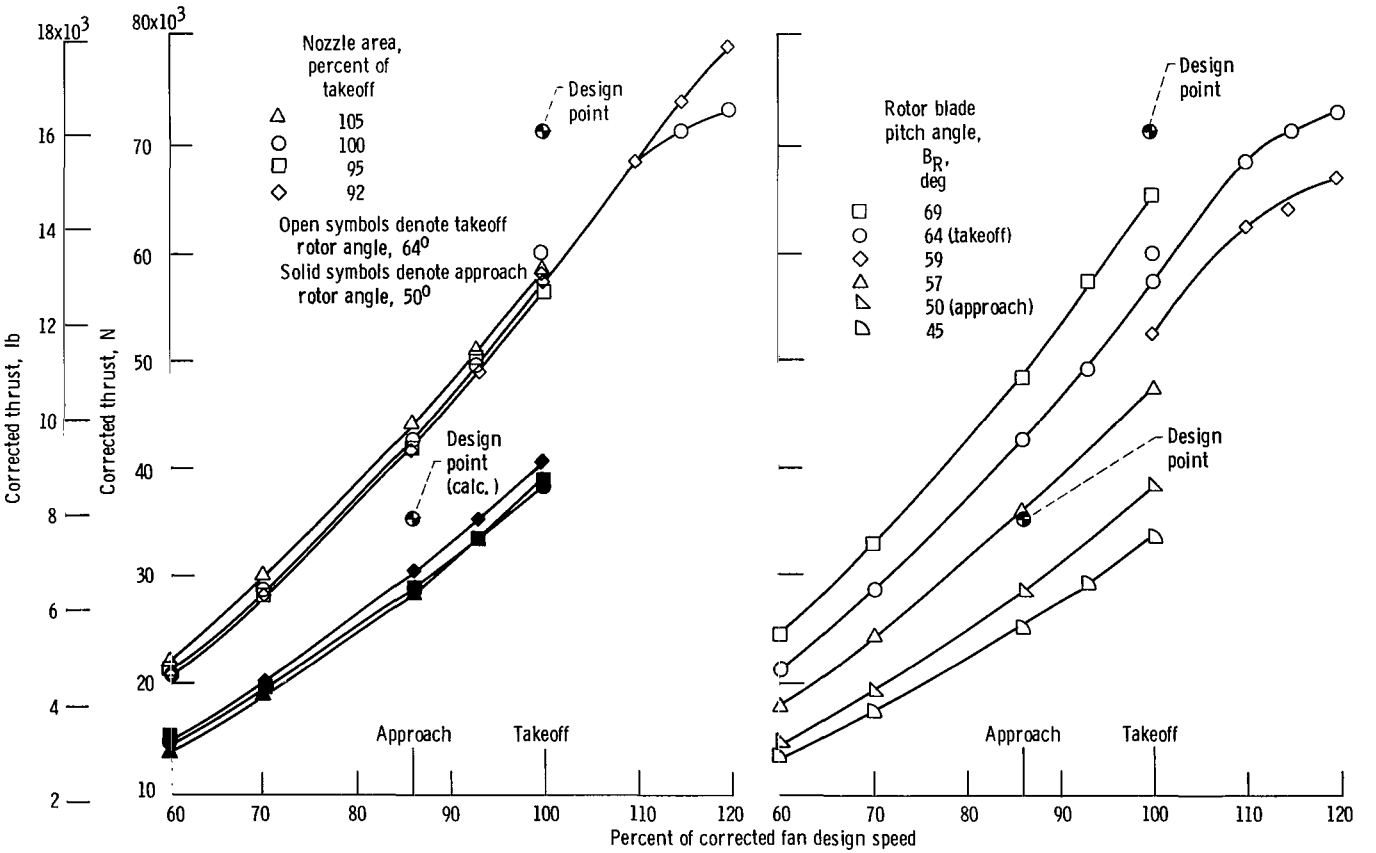

(a) For two rotor blade pitch angles and four nozzle areas.

(b) For six rotor blade pitch angles at design nozzle area.

Figure 14. - Corrected thrust as function of percent of corrected fan design speed.

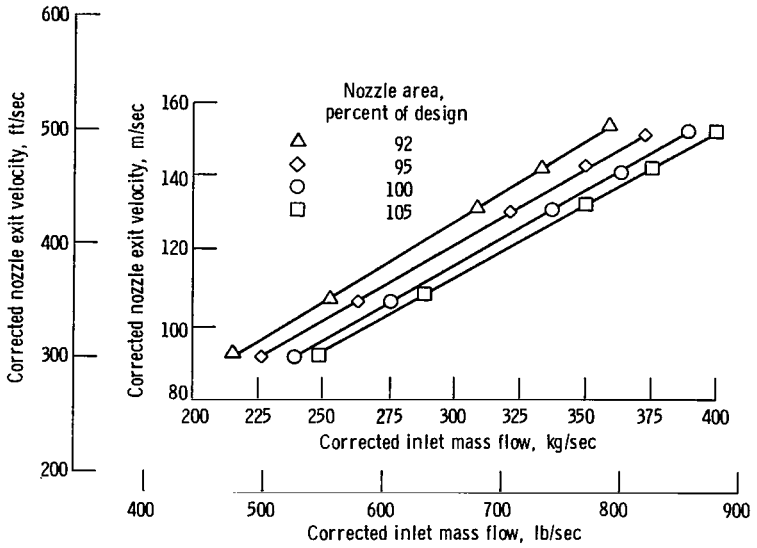

Figure 15. - Corrected nozzle exit velocity as function of corrected inlet mass flow. Design (takeoff) rotor angle, 64^{0}.

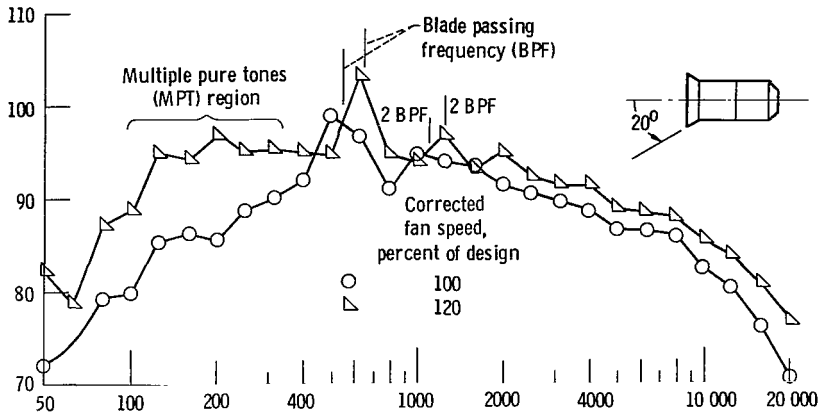

(a) One-third-octave spectra. Bandwidth, 32 hertz.

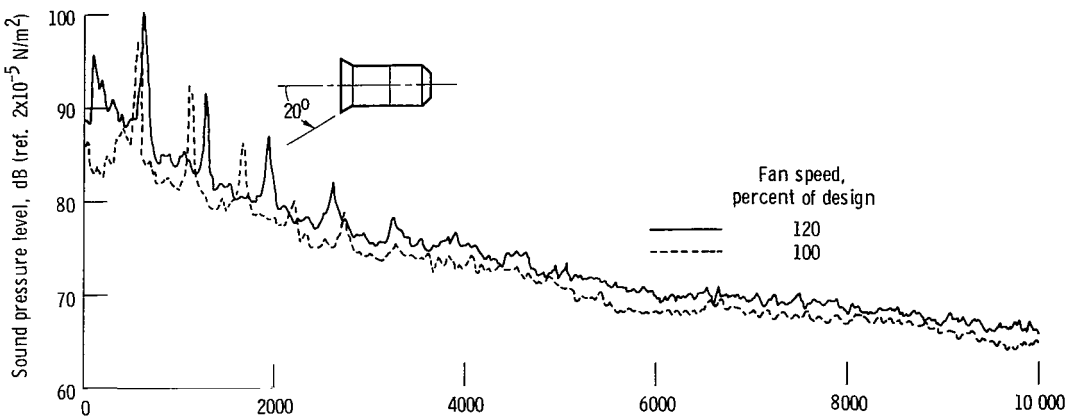

(b) Comparison of narrow-band spectra. Bandwidth, 32 hertz.

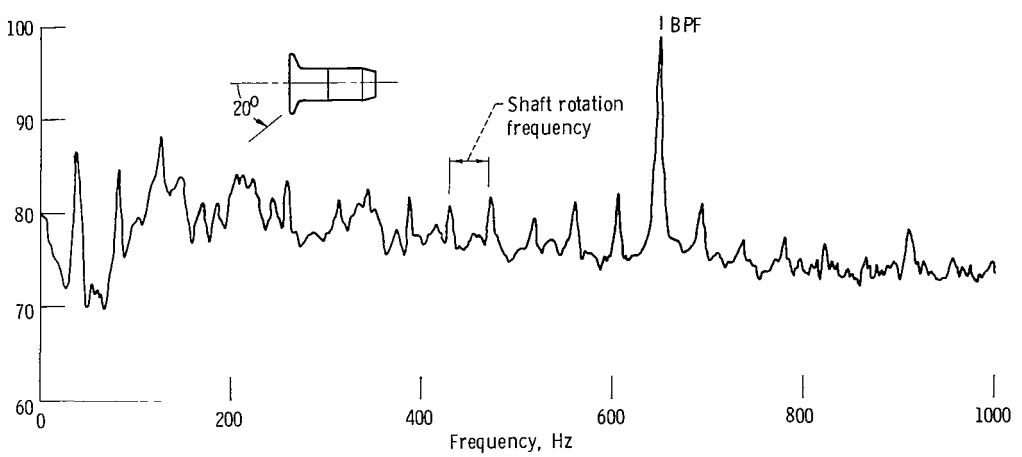

(c) Low frequency detail of multiple pure tone spectra. Bandwidth, 3.2 hertz; tip speed, 256 meters per second (840 ft/sec).

Figure 16. - Sound pressure level spectra at 20° from inlet axis on 30.5-meter (100-ft) radius. Design (takeoff) rotor angle, 64°; design nozzle area.

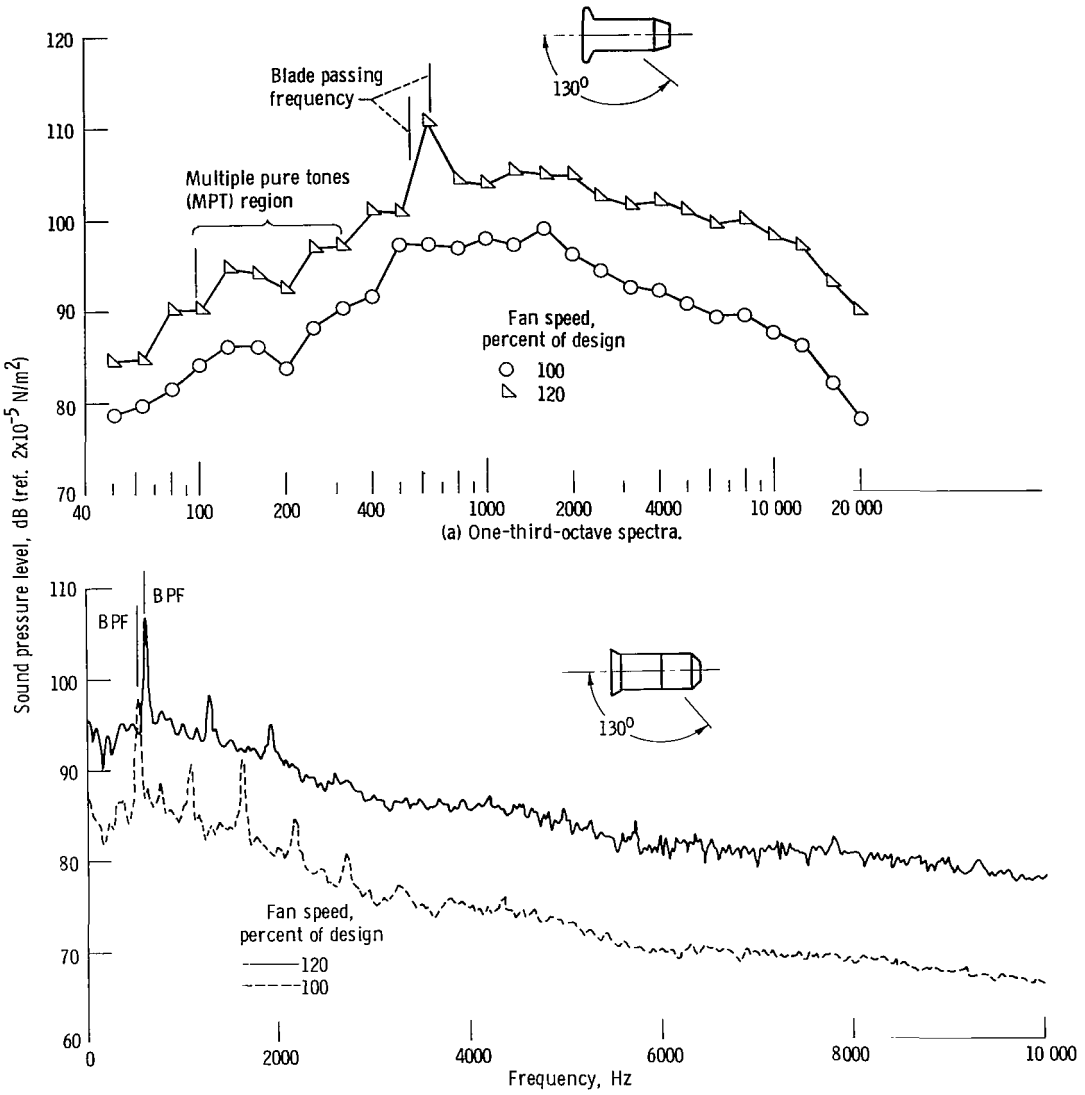

(b) Comparison of narrow-band spectra. Bandwidth, 32 hertz.

Figure 17. - Sound pressure level spectra at 130^0 from inlet on 30.5-meter (100-ft) radius. Design (takeoff) rotor angle, 64^0; design nozzle area.

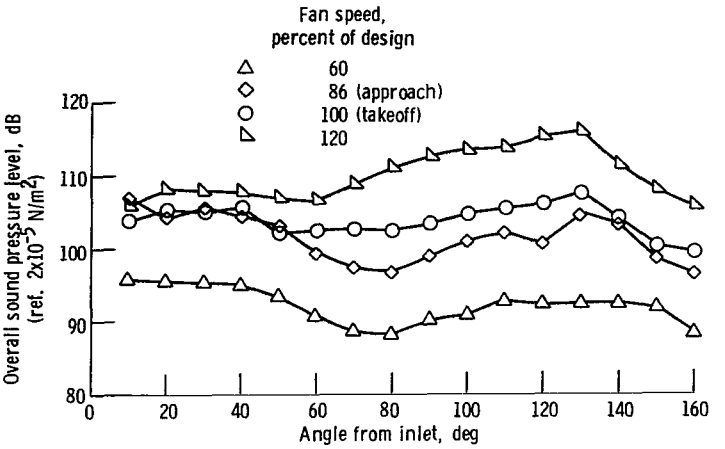

Figure 18. - Effect of fan speed on overall sound pressure level on 30.5 meter (100 ft) radius. Design (takeoff) rotor angle, 64°; design nozzle area.

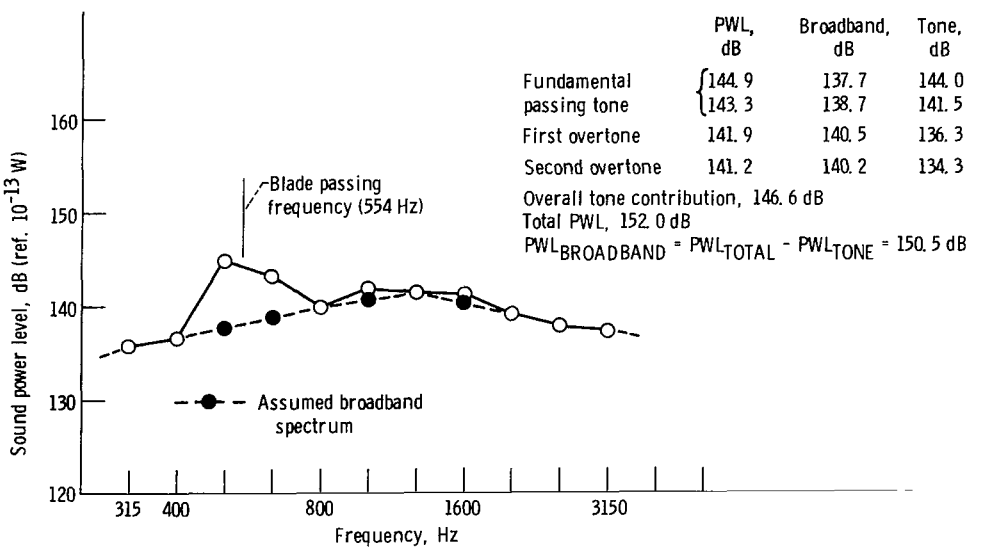

Figure 19. - Separated pure tone and broadband sound pressure and power levels in one-third-octave spectra. Data shown for takeoff configuration at design speed.

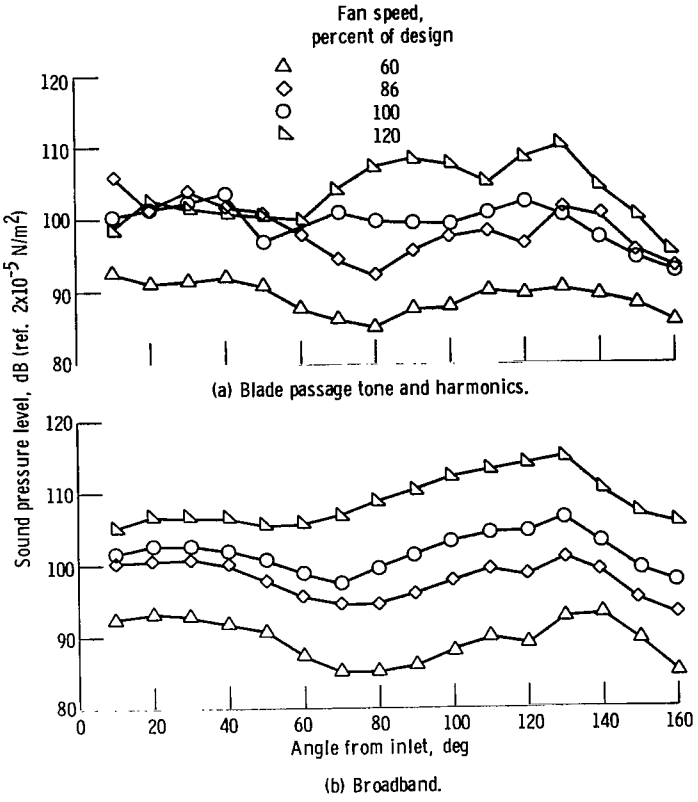

Figure 20. - Angular distribution of noise components on 30.5-meter (100-ft) radius. Takeoff configuration.

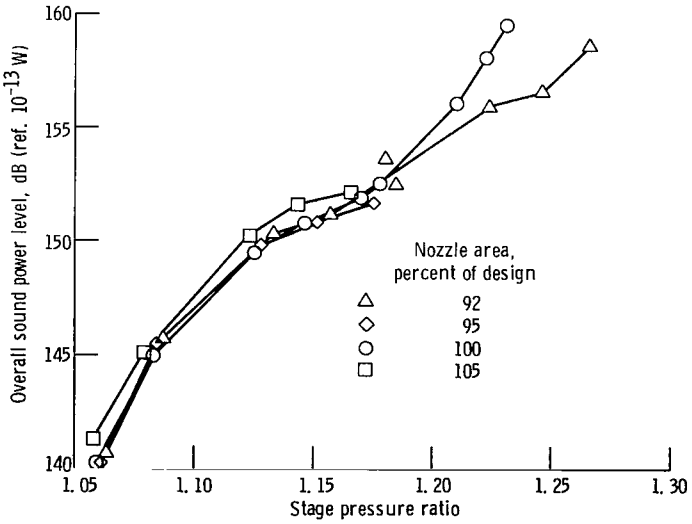

Figure 21. - Overall sound power level as function of stage pressure ratio. Design (takeoff) rotor angle, 64°.

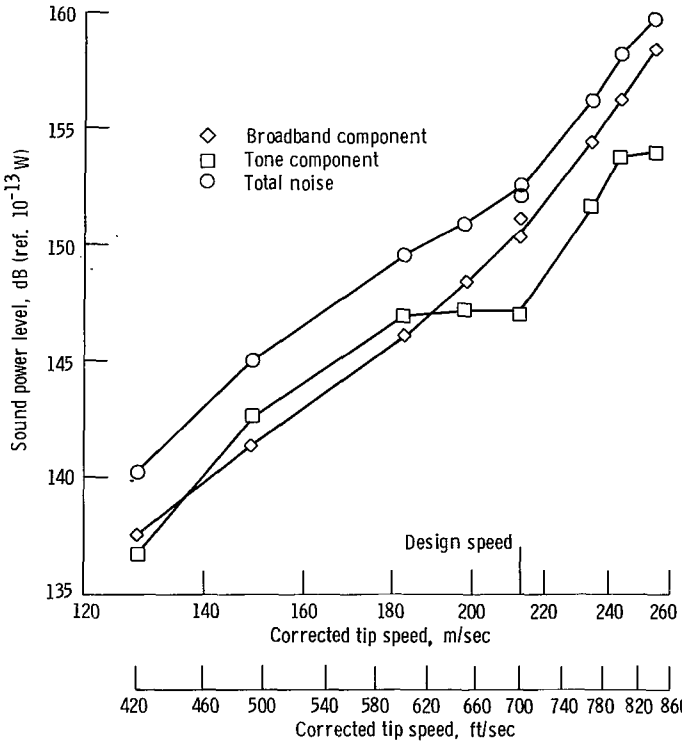

Figure 22. - Fan speed effect on sound power noise components. Design (takeoff) rotor angle, 64^{0}; design nozzle area.

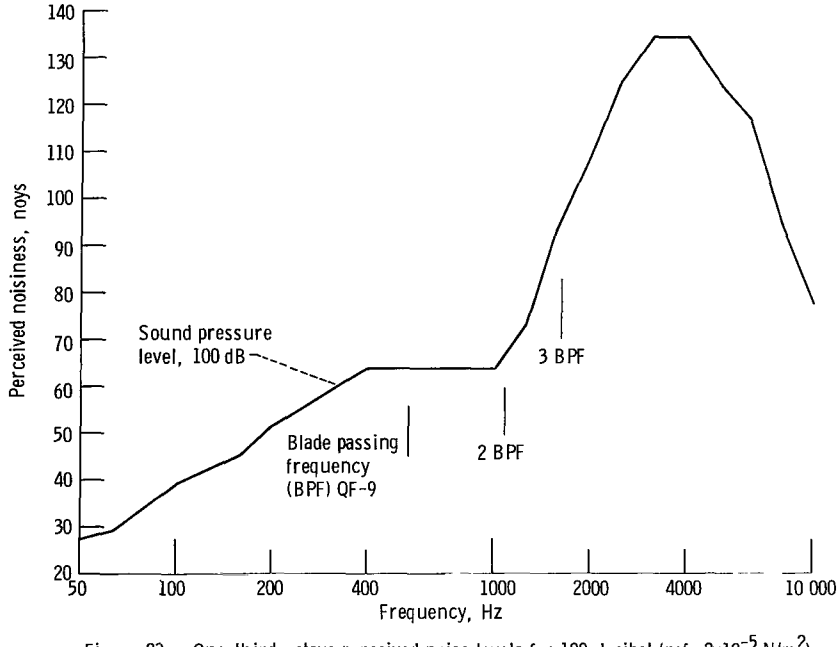

Figure 23. - One-third-octave perceived noise levels for 100-decibel (ref. $2x10^{-5}$ N/m^2) sound pressure level at all frequencies.

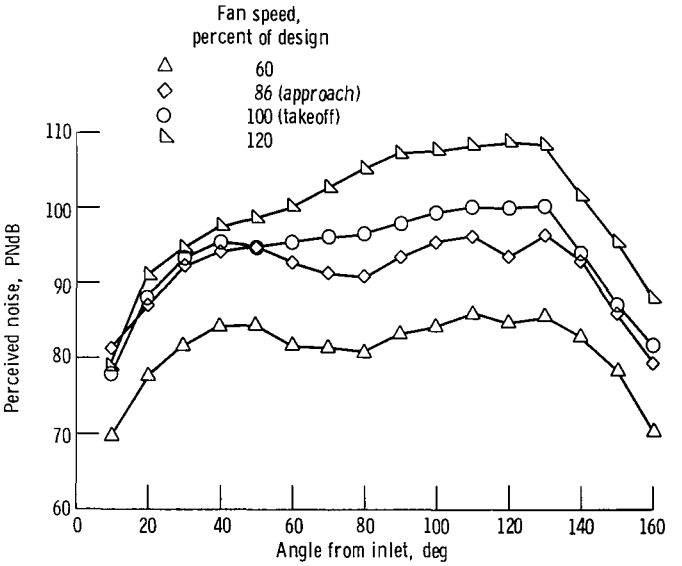

Figure 24. - Effect of fan speed on perceived noise along 152.4-meter (500-ft) sideline. Design (takeoff) rotor angle, 64°; design nozzle area.

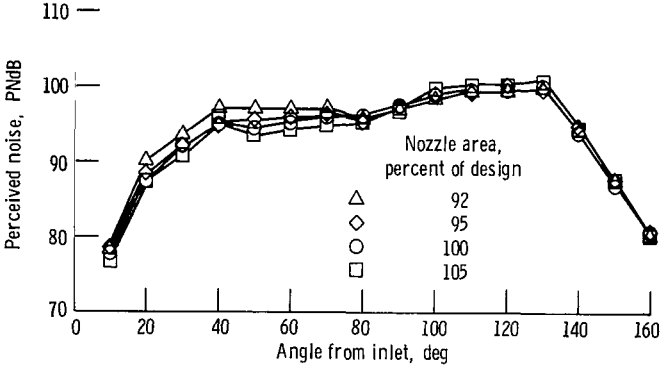

Figure 25. - Effect of nozzle area on perceived noise along 152.4-meter (500-ft) sideline. Design (takeoff) rotor angle, 64°; design fan speed.

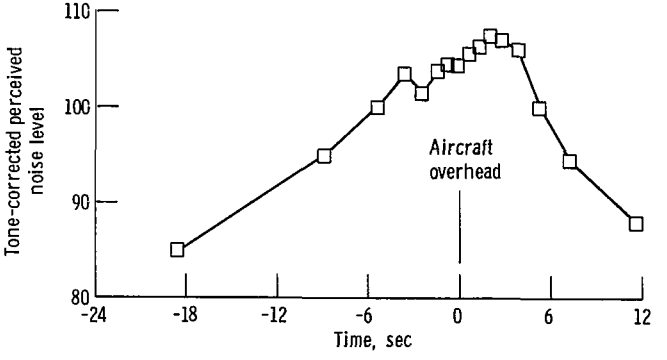

Figure 26. - Flyover noise history for four-engine STOL aircraft at 152.4-meter (500 ft) altitude. Aircraft velocity, 41 meters per second (135 ft/sec); effective perceived noise level, 105.2 EPNdB; design nozzle area and fan speed (no relative velocity effects).

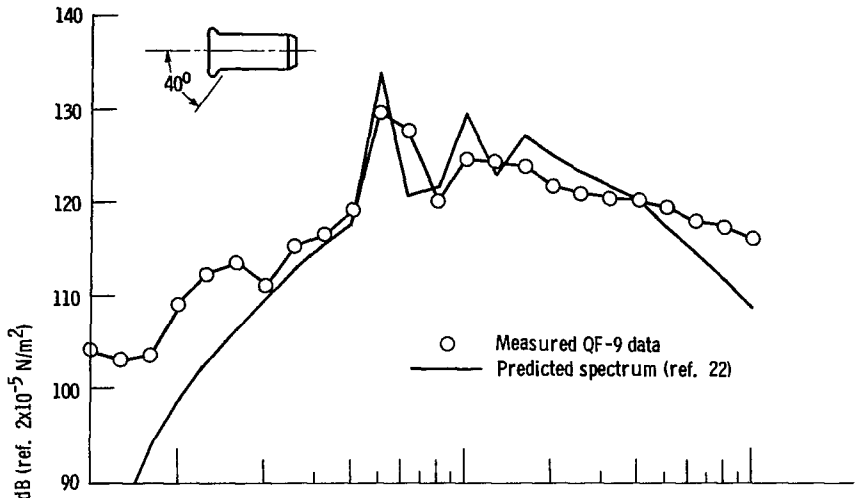

(a) Sound pressure level at 1-meter radius, 40° from inlet.

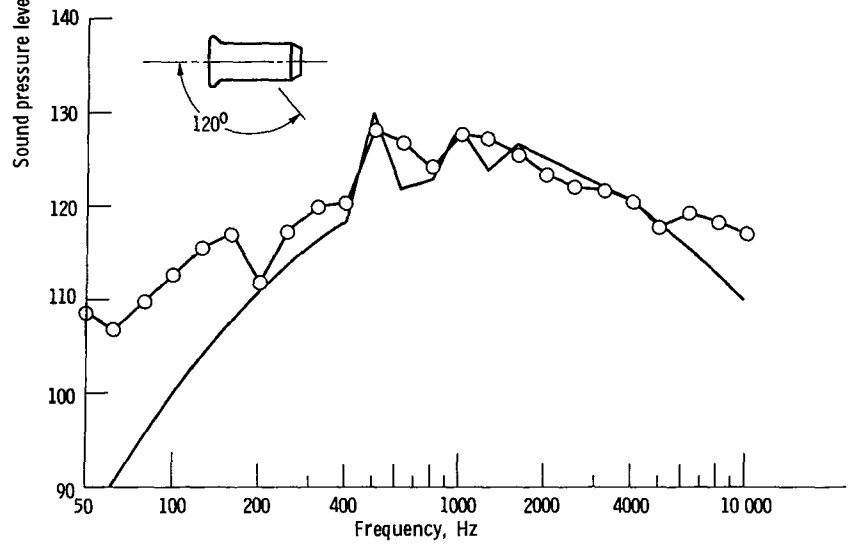

(b) Sound pressure level at 1-meter radius, 120° from inlet.

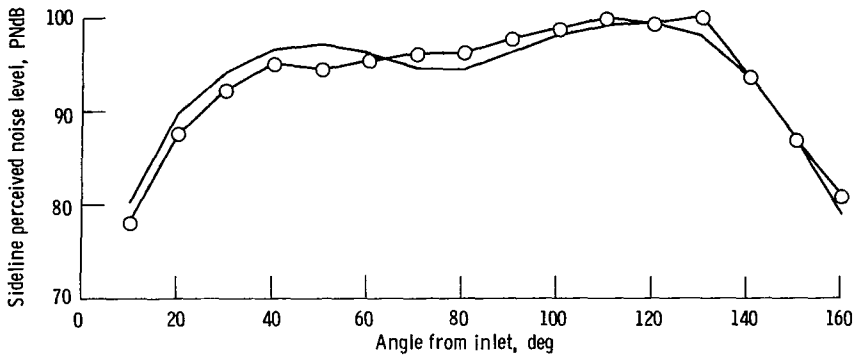

(c) Perceived noise level along 152.4-meter (500 ft) sideline.

Figure 27. - Comparison of fan noise predicted data to measure QF-9 data for takeoff design configuration and design speed.

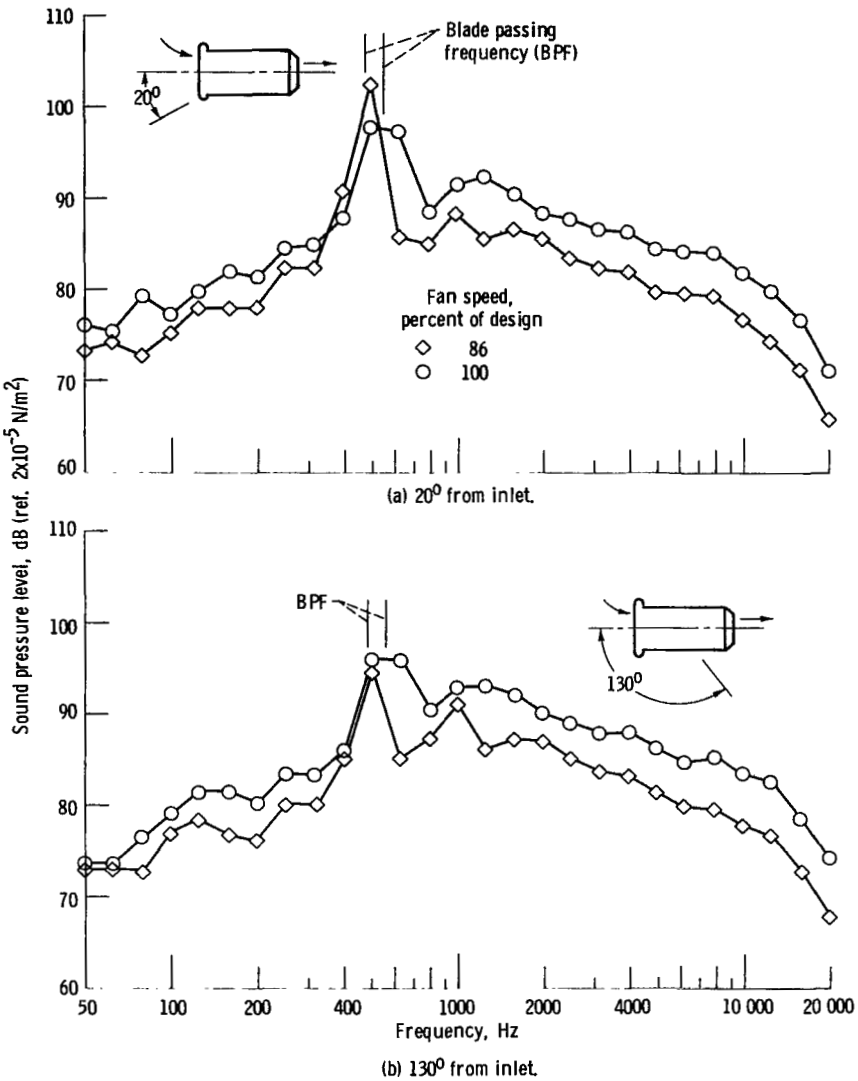

Figure 28. - One-third-octave sound pressure level spectra on 30.5-meter (100-ft) radius. Design (approach) rotor angle, 50°; design nozzle area.

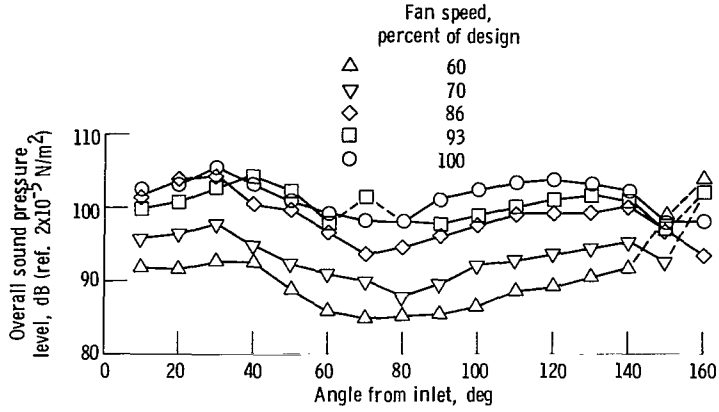

Figure 29. - Effect of fan speed on overall sound pressure level on 30.5-meter (100 ft) radius. Design (approach) rotor angle, 50°; design nozzle area.

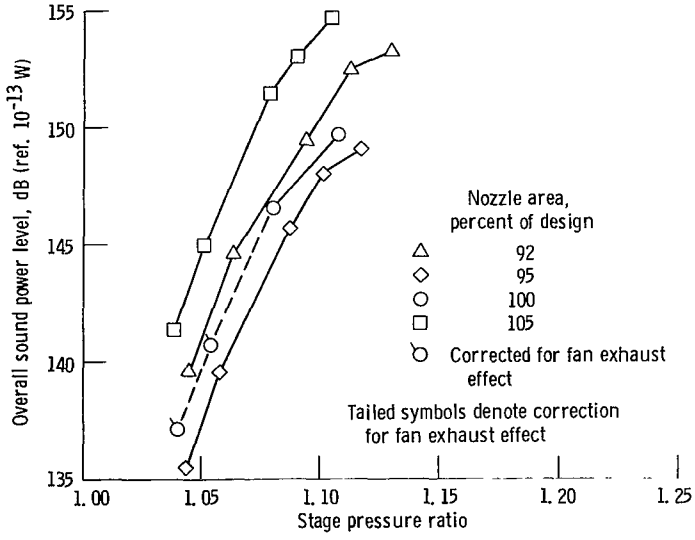

Figure 30. - Overall sound power level as function of stage pressure ratio. Design (approach) rotor angle, 50°.

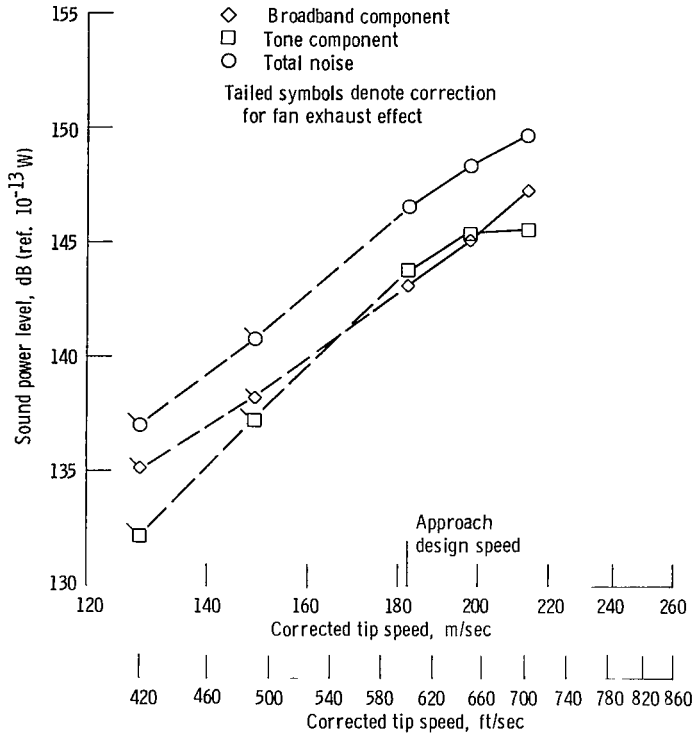

Figure 31. - Fan speed effect on sound power noise components. Approach rotor angle; design nozzle area.

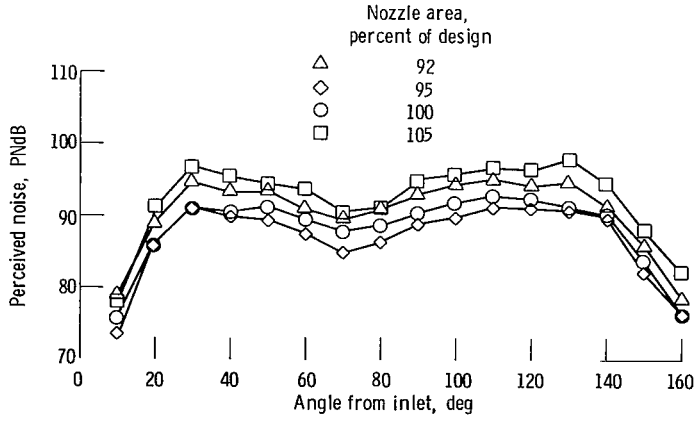

Figure 32. - Perceived noise level on 152.4-meter (500-ft) sideline. Approach design speed, 86 percent of design; approach rotor angle.

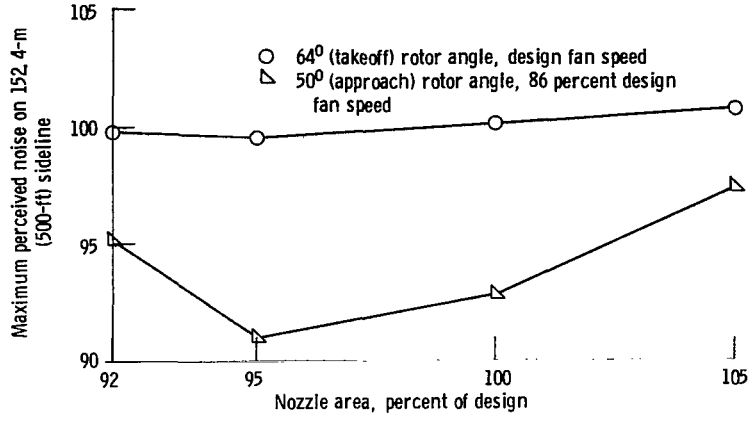

Figure 33. - Maximum perceived noise along 152.4-meter (500-ft) sideline as function of nozzle area.

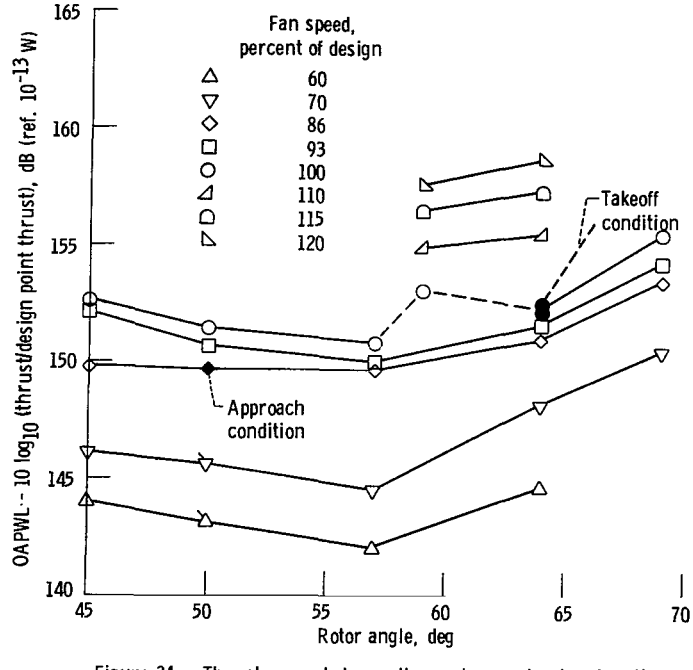

Figure 34. - Thrust-corrected overall sound power level as function of rotor angle for design nozzle area.

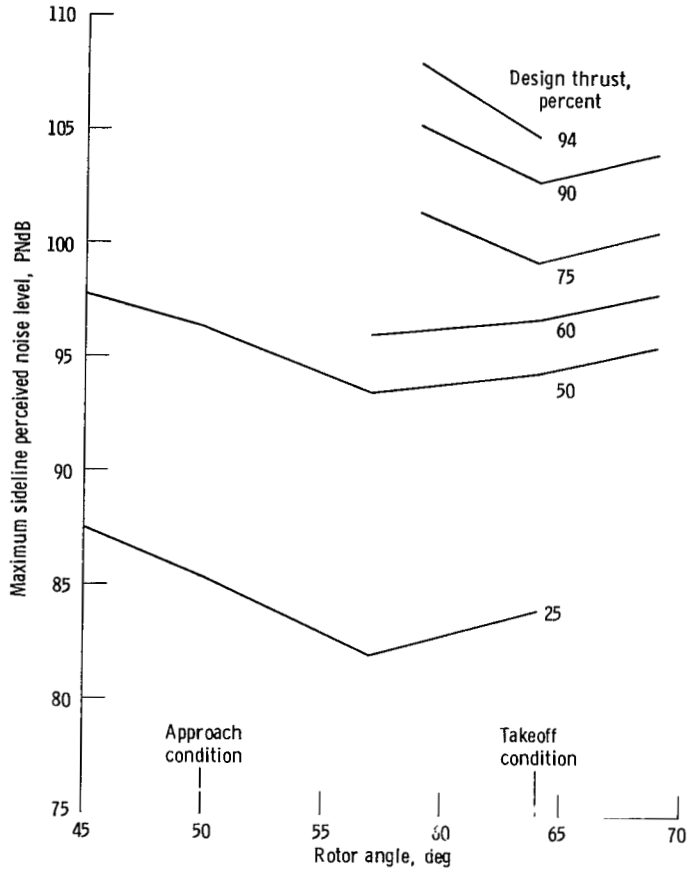

Figure 35. - Maximum sideline perceived noise level along 152.4-meter (500-ft) sideline for constant thrust conditions as function of rotor angle for design nozzle area.

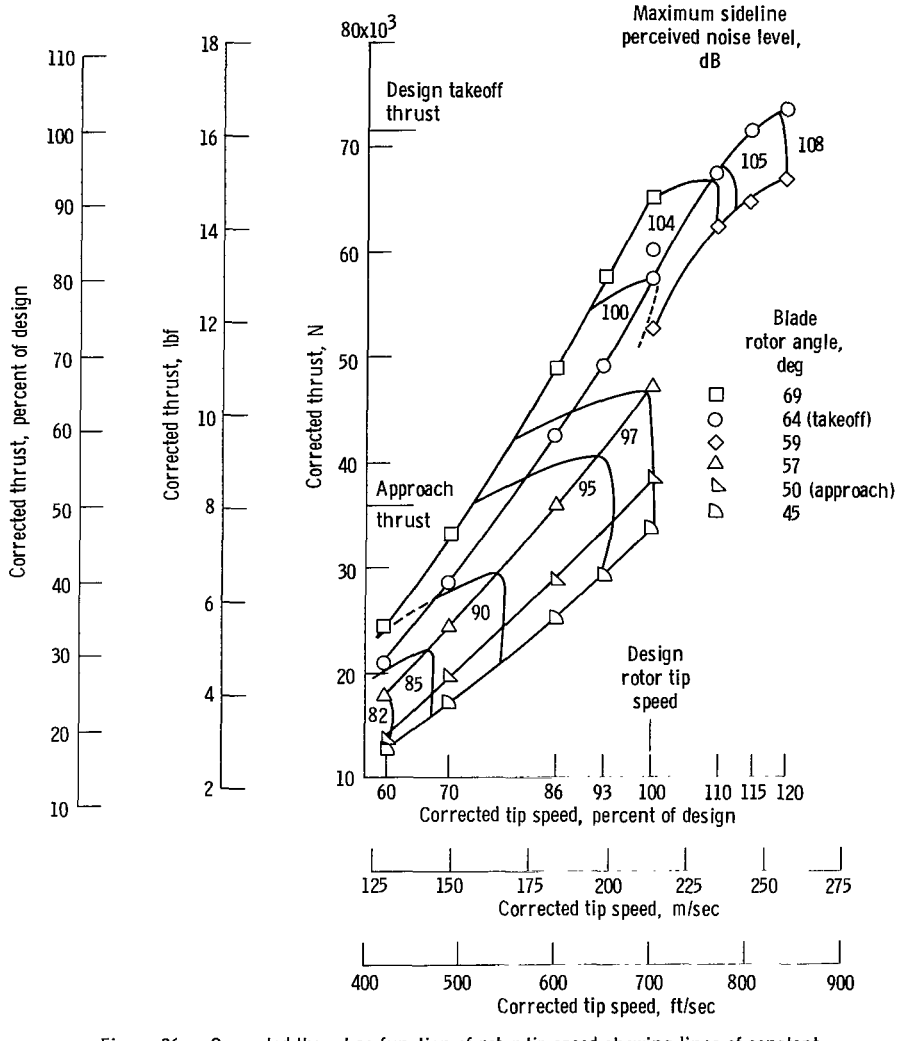

Figure 36. - Corrected thrust as function of rotor tip speed showing lines of constant perceived noise level on 152.4-meter (500 ft) sideline with design nozzle area.

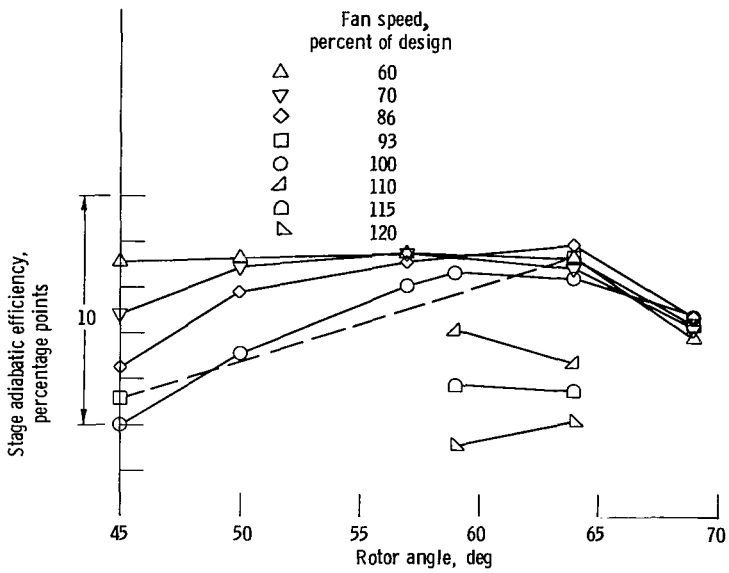

Figure 37. - Stage adiabatic efficiency as function of rotor pitch angle. Design nozzle area.

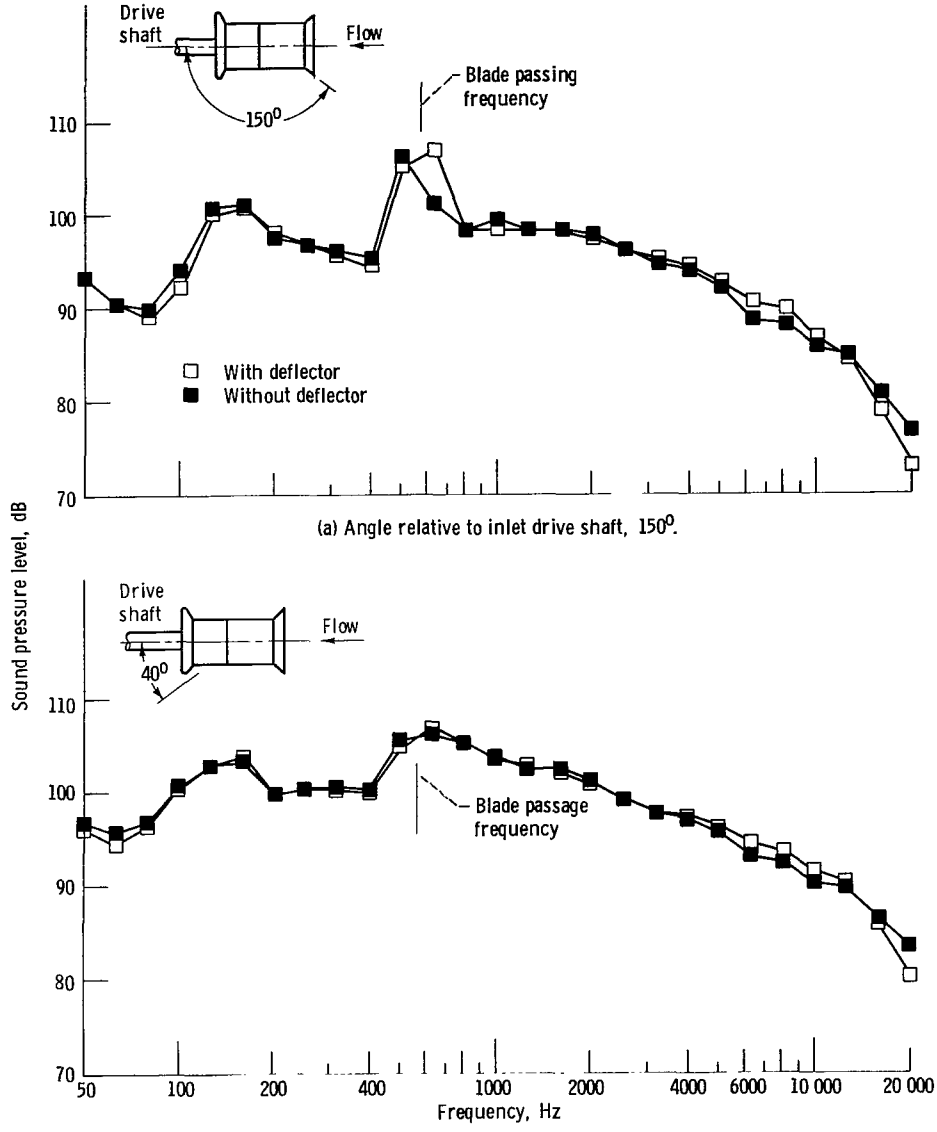

(a) Angle relative to inlet drive shaft, 150°.

(b) Angle relative to inlet drive shaft, 40°.

Figure 38. - One-third-octave sound pressure level spectra on 30.5-meter (100-ft) radius. Reverse configuration; design speed.

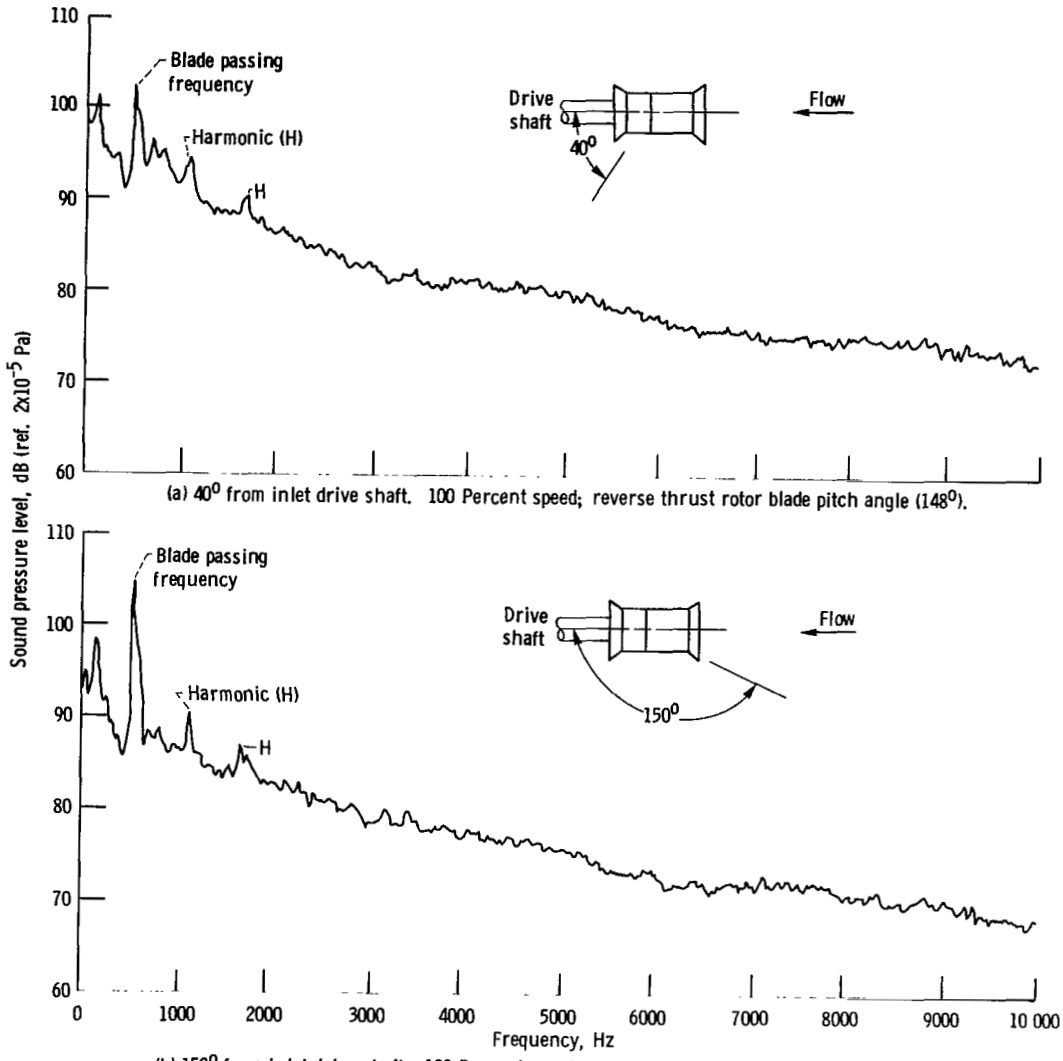

(a) 40° from inlet drive shaft. 100 Percent speed; reverse thrust rotor blade pitch angle (148°).

(b) 150° from inlet drive shaft. 100 Percent speed; reverse thrust rotor blade pitch angle (148°).

Figure 39. - Narrow band spectra (32-Hz bandwidth) on 30.5-meter (100-ft) radius.

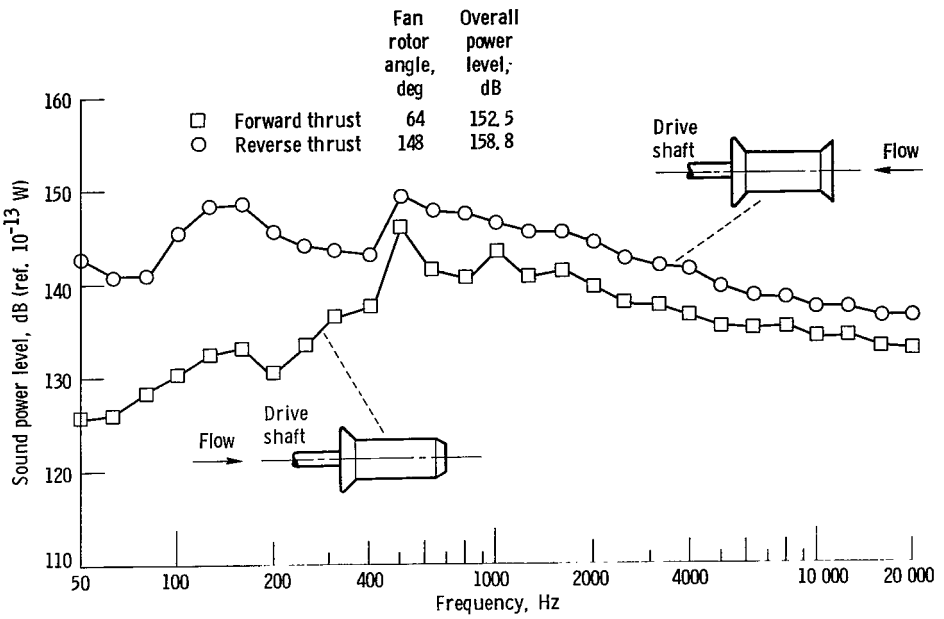

Figure 40. - Comparison of design configuration forward thrust (B_R = 64°) and reverse thrust (B_R = 148°) sound power level spectra with design fan speed.

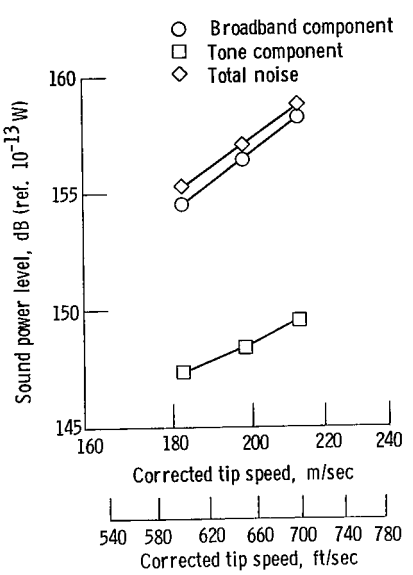

Figure 41. - Fan speed effect on sound power noise components for reverse thrust rotor angle (148°).

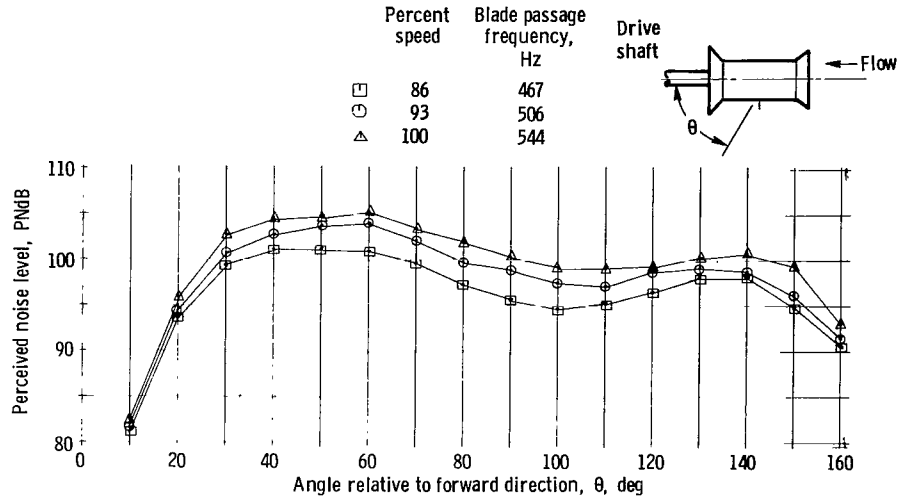

Figure 42. - Perceived noise on 152.5-meter (500-ft) sideline with reverse thrust rotor blade pitch angle (148°).

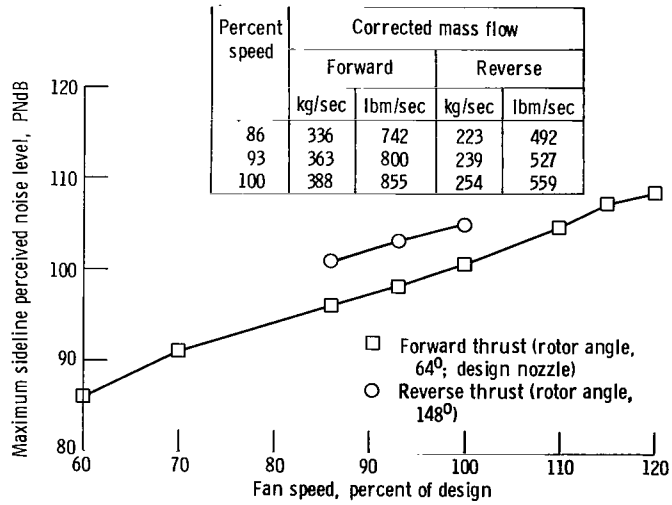

Figure 43. - Maximum perceived noise level on 152.4-meter (500-ft) sideline as function of percent of design speed.

NATIONAL AERONAUTICS AND SPACE ADMINISTRATION
WASHINGTON, D.C. 20546

OFFICIAL BUSINESS
PENALTY FOR PRIVATE USE $300

SPECIAL FOURTH-CLASS RATE
BOOK

POSTAGE AND FEES PAID
NATIONAL AERONAUTICS AND
SPACE ADMINISTRATION
451

U.S.MAIL

109 001 C1 U A 770204 S00903DS
DEPT OF THE AIR FORCE
AF WEAPONS LABORATORY
ATTN: TECHNICAL LIBRARY (SUL)
KIRTLAND AFB NM 87117

POSTMASTER: If Undeliverable (Section 158 Postal Manual) Do Not Return

"The aeronautical and space activities of the United States shall be conducted so as to contribute . . . to the expansion of human knowledge of phenomena in the atmosphere and space. The Administration shall provide for the widest practicable and appropriate dissemination of information concerning its activities and the results thereof."

—NATIONAL AERONAUTICS AND SPACE ACT OF 1958

NASA SCIENTIFIC AND TECHNICAL PUBLICATIONS

TECHNICAL REPORTS: Scientific and technical information considered important, complete, and a lasting contribution to existing knowledge.

TECHNICAL NOTES: Information less broad in scope but nevertheless of importance as a contribution to existing knowledge.

TECHNICAL MEMORANDUMS: Information receiving limited distribution because of preliminary data, security classification, or other reasons. Also includes conference proceedings with either limited or unlimited distribution.

CONTRACTOR REPORTS: Scientific and technical information generated under a NASA contract or grant and considered an important contribution to existing knowledge.

TECHNICAL TRANSLATIONS: Information published in a foreign language considered to merit NASA distribution in English.

SPECIAL PUBLICATIONS: Information derived from or of value to NASA activities. Publications include final reports of major projects, monographs, data compilations, handbooks, sourcebooks, and special bibliographies.

TECHNOLOGY UTILIZATION PUBLICATIONS: Information on technology used by NASA that may be of particular interest in commercial and other non-aerospace applications. Publications include Tech Briefs, Technology Utilization Reports and Technology Surveys.

Details on the availability of these publications may be obtained from:

SCIENTIFIC AND TECHNICAL INFORMATION OFFICE

NATIONAL AERONAUTICS AND SPACE ADMINISTRATION

Washington, D.C. 20546